Stem Cell Reports
Article

ISSCR

OPEN ACCESS

Connexin 43-Mediated Mitochondrial Transfer of iPSC-MSCs Alleviates Asthma Inflammation

Yin Yao,[1,5] Xing-Liang Fan,[1,5] Dan Jiang,[2,3,5] Yuelin Zhang,[4] Xin Li,[4] Zhi-Bin Xu,[1] Shu-Bin Fang,[1] Sinming Chiu,[2,3] Hung-Fat Tse,[2] Qizhou Lian,[2,3,*] and Qing-Ling Fu[1,*]

[1]Otorhinolaryngology Hospital, The First Affiliated Hospital, Sun Yat-sen University, 58 Zhongshan Road II, Guangzhou 510080, P. R. China
[2]Department of Medicine, The University of Hong Kong, Hong Kong SAR, P. R. China
[3]Stem Cell and Regenerative Medicine Consortium, The University of Hong Kong, Hong Kong SAR, P. R. China
[4]Department of Emergency, Guangdong General Hospital, Guangdong Academy of Medical Sciences, 106 Zhongshan Road II, Guangzhou 510080, P. R. China
[5]Co-first author
*Correspondence: qzlian@hku.hk (Q.L.), fuqingl@mail.sysu.edu.cn (Q.-L.F.)
https://doi.org/10.1016/j.stemcr.2018.09.012

SUMMARY

We previously identified an immunomodulatory role of human induced pluripotent stem cell (iPSC)-derived mesenchymal stem cells (MSCs) in asthmatic inflammation. Mitochondrial transfer from bone marrow MSCs to epithelial cells can result in the attenuation of acute lung injury in mice. However, the effects of mitochondrial transfer from iPSC-MSCs to epithelial cells in asthma and the mechanisms underlying these effects are unclear. We found that iPSC-MSC transplantation significantly reduced T helper 2 cytokines, attenuated the mitochondrial dysfunction of epithelial cells, and alleviated asthma inflammation in mice. Tunneling nanotubes (TNTs) were formed between iPSC-MSCs and epithelial cells, and mitochondrial transfer from iPSC-MSCs to epithelial cells via TNTs was observed both *in vitro* and in mice. Overexpression or silencing of connexin 43 (CX43) in iPSC-MSCs demonstrated that CX43 plays a critical role in the regulation of TNT formation by mediating mitochondrial transfer between iPSC-MSCs and epithelial cells. This study provides a therapeutic strategy for targeting asthma inflammation.

INTRODUCTION

Asthma, one of the most common chronic diseases, especially among children, is a complex inflammatory disorder characterized by chronic and persistent inflammation of the airways (Lambrecht and Hammad, 2015). Currently, asthma affects more than 300 million people worldwide, especially in developing countries (Poole, 2014; Zar and Levin, 2012). Despite advances in pharmacological therapy, the prevalence of asthma is increasing steeply. Over the past decades, the mechanisms underlying the pathogenesis of asthma have been intensively studied, and epithelial cell injury is considered to be a major cause of asthma (Lambrecht and Hammad, 2012). It has been reported that mitochondrial dysfunction causes airway epithelial cell injury and apoptosis, leading to allergic airway inflammation (Chan et al., 2017; Plotkowski et al., 2002; Spees et al., 2006). Given the accumulating evidence linking mitochondrial injury and inflammation, targeting mitochondrial dysfunction of epithelial cells may be a strategy for asthma therapy.

An increasing number of studies have demonstrated that mesenchymal stem cell (MSC)-based therapy shows promising results for allergic airway inflammation (Cruz et al., 2015; Dai et al., 2017; Takeda et al., 2018). We have demonstrated that MSCs derived from induced pluripotent stem cells (iPSC-MSCs) not only effectively inhibit allergic airway inflammation and alleviate asthma in a mouse model but also modulate T cell phenotypes in allergic rhinitis patients (Fu et al., 2012; Sun et al., 2012), indicating that iPSC-MSC-based therapy could be relevant to the treatment of allergic airway inflammation. MSCs derived from adult tissues, such as bone marrow (BM), have limited proliferative capacities and exhibit great variability in cell quality across different donors, which limits their therapeutic benefits, especially in clinical applications (Crisostomo et al., 2006). We previously found that iPSC-MSCs had lower immunogenicity and superior survival and engraftment following transplantation in a mouse ischemia model compared with BM-MSCs (Sun et al., 2015). We also reported that iPSC-MSCs have a better cell proliferation ability, longer life span (more than 50 passages), and less cell senescence than BM-MSCs (Gao et al., 2017; Lian et al., 2010). Recent studies have demonstrated that BM-MSCs exert beneficial effects via mitochondrial transfer in mouse models of acute lung injury and allergic airway inflammation (Ahmad et al., 2014; Islam et al., 2012). We previously reported that mitochondrial transfer from iPSC-MSCs to airway epithelial cells and airway smooth muscle cells mainly occurs via tunneling nanotubes (TNTs) to rescue lung injury induced by cigarette smoke or oxidative stress agents (Li et al., 2014, 2018). Nevertheless, whether the alleviation of asthma inflammation by iPSC-MSCs is attributed to mitochondria donation and the possible mechanisms of this effect remain unclear.

Connexin 43 (CX43), a gap junction protein that regulates a cell connection channel or TNTs, mediates organelle exchange or migration between cells. BM-MSCs were demonstrated to protect against acute lung injury via CX43-mediated mitochondrial donation to alveoli, suggesting that CX43 plays a prominent role in regulating mitochondrial transfer (Islam et al., 2012). Additionally, we reported that CX43 is upregulated in mouse lungs during asthma (Yao et al., 2015), which is essential for mitochondrial transfer. Therefore, we hypothesized that CX43-regulated TNT formation is important for mitochondrial transfer from iPSC-MSCs to the injured bronchial epithelial cells, thereby inhibiting asthma inflammation.

In this study, we found that local transplantation of iPSC-MSCs alleviated airway inflammation and rescued mitochondrial dysfunction in a mouse model of asthma. We observed that CX43 regulated TNT formation between iPSC-MSCs and epithelial cells *in vitro* and further observed that iPSC-MSCs donated the mitochondria to the dysfunctional mitochondrial epithelial cells in mice and *in vitro*. Notably, we showed that CX43 contributes to mitochondrial transfer via regulating TNT formation in iPSC-MSCs.

RESULTS

Local Transplantation of iPSC-MSCs Alleviates Ovalbumin-Induced Asthma Inflammation in Mice

We previously reported that intravenous injection of iPSC-MSCs prevented allergic airway inflammation in mice (Sun et al., 2012). To investigate the effects of iPSC-MSCs on epithelial cells, two clones of iPSC-MSCs were intratracheally administered in a mouse model of asthma. Compared with that in the control group, the administration of ovalbumin (OVA) significantly increased lung inflammatory infiltration, indicating the successful establishment of an asthma animal model (Figure 1A). H&E and periodic acid–Schiff (PAS) staining showed that, compared with the OVA group, local transplantation of N1-iPSC-MSCs and iMR90-iPSC-MSCs significantly alleviated peribronchial and perivessel inflammation and decreased mucus secretion in hyperplastic goblet cells (Figure 1A). The inflammation score and mucus hypersecretion were significantly decreased by more than 50% in the N1-iPSC-MSC and iMR90-iPSC-MSC groups compared with those in the OVA group (Figure 1B, $p < 0.01$). Administration of iPSC-MSCs significantly alleviated the airway hyperresponsiveness at different methacholine concentrations (6.25, 12.5, 25, 50, and 100 mg/mL) (Figure S1). Furthermore, eosinophils, macrophages, lymphocytes, neutrophils, and total inflammatory cells in the bronchoalveolar lavage fluid (BALF) were greatly reduced in the N1-iPSC-MSC and iMR90-iPSC-MSC groups compared with those in the OVA group (Figure 1C). Similarly, the T helper 2 (Th2) cytokine (interleukin [IL]-4, IL-5, and IL-13) levels in BALF, immunoglobulin (Ig) E levels in serum, and epithelium-derived cytokine (IL-33 and thymic stromal lymphopoietin [TSLP]) levels in lung homogenates were much lower in the iPSC-MSC-treated group than in the OVA group (Figures 1D–1F, $p < 0.001$). Therefore, local transplantation of iPSC-MSCs significantly alleviates asthma inflammation induced by OVA in mice.

iPSC-MSCs Effectively Reduce OVA-Induced Mitochondrial Dysfunction in the Lung

We next investigated the survival and distribution of iPSC-MSCs post transplantation. The engraftment of GFP-transfected iPSC-MSCs (GFP-iPSC-MSCs) was detected by fluorescence microscopy and flow cytometry at different time points (1 hr, 4 hr, 8 hr, 24 hr, and 96 hr). We observed the survival and distribution of GFP-iPSC-MSCs in the lung at 1 and 4 hr after transplantation in both the OVA group and the PBS group. The number of GFP-iPSC-MSCs gradually decreased in a time-dependent manner and disappeared after 1 day in the PBS group. However, some GFP-iPSC-MSCs were still detected in the lungs even at 4 days after transplantation in the OVA-treated mice (Figure 2A). These results were further verified by flow cytometry. One hour after transplantation, more than 6% of GFP^+ cells in the cell population were detected in both the OVA group and the PBS group. Although the percentage of GFP^+ cells declined over time, engrafted cells were still detected up to 4 days later in the OVA-treated mice, suggesting that the engraftment of iPSC-MSCs into the lungs of OVA-treated mice was much higher than that in the lungs of controls (Figure 2B).

To further determine the effects of iPSC-MSCs on epithelial mitochondrial function, scanning transmission electron microscopy (TEM) and flow cytometry were performed to examine the morphological and functional changes in the epithelial mitochondria. These analyses showed that the administration of OVA led to swollen mitochondria (Figure 2C) and a decreased mitochondrial inner membrane potential in the lung (Figures 2D and 2E, $p < 0.001$), whereas iPSC-MSC treatment improved the mitochondrial morphology and partially restored the mitochondrial inner membrane potential to a level similar to that in the PBS group (Figures 2C–2E). In addition, western blot analysis showed that the administration of OVA elevated the levels of caspase 3, caspase 9, and their cleaved products in lung tissue. In contrast, transplantation of iPSC-MSCs significantly reduced the expression of

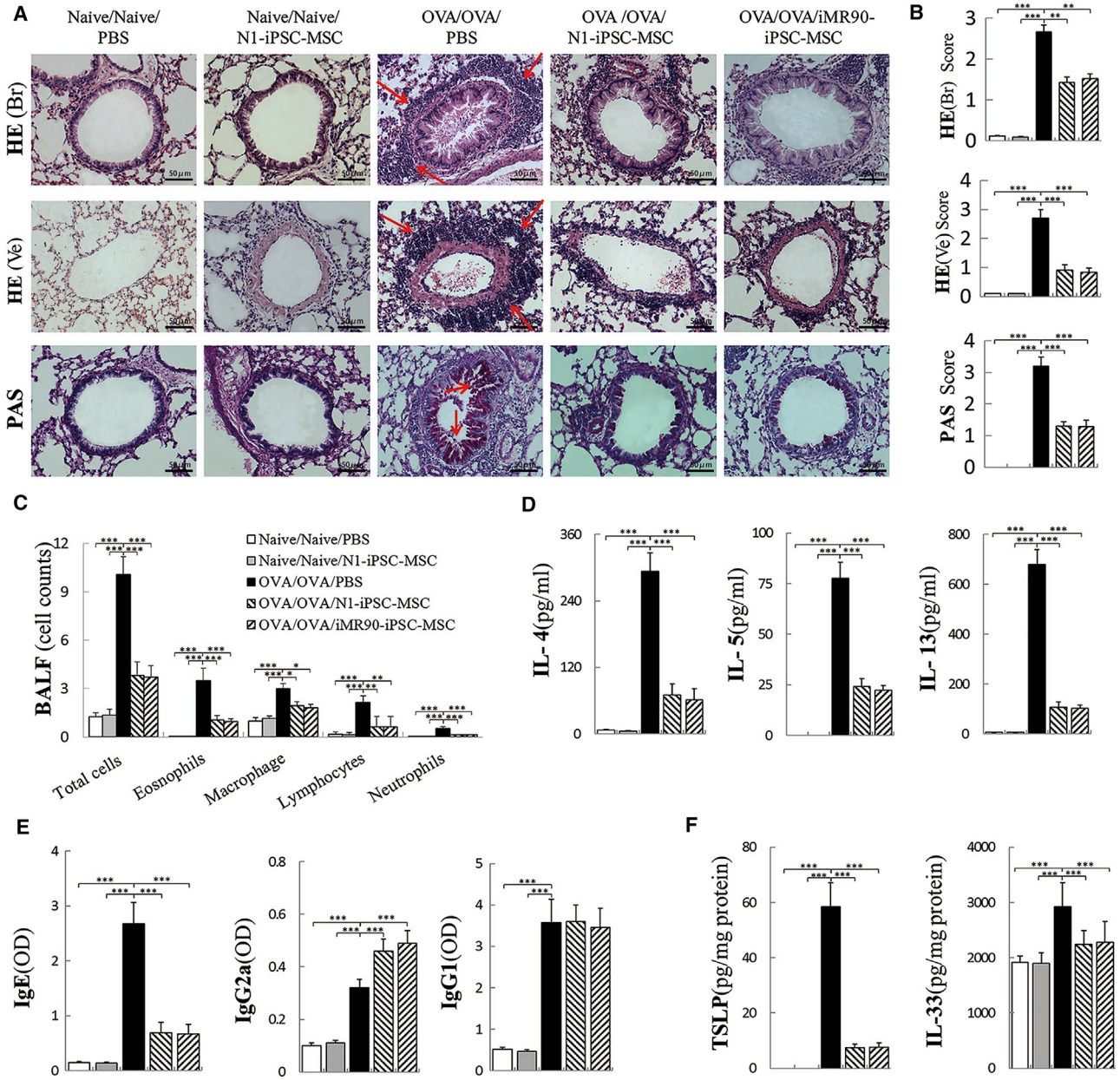

Figure 1. Transplantation of iPSC-MSCs Significantly Alleviates Asthma Inflammation via Local Application in Mice

(A) Representative photomicrographs of H&E- and PAS-stained lung sections from each group showing inflammatory infiltrates (lung H&E, shown by arrows) and mucus accumulation at the luminal surface of the bronchi (lung PAS staining, shown by arrows) in lungs from different groups.

(B) Statistical analysis of the inflammation score and mucus hypersecretion as quantified by H&E/PAS staining (n = 6).

(C–F) The inflammatory cell counts in BALF (C, n = 6); cytokine IL-4, IL-5, and IL-13 levels in BALF (D, n = 6); IgE, IgG1, and IgG2a levels in serum (E, n = 6); and TSLP and IL-33 levels in lung homogenates (F, n = 6) were measured using ELISA.

Data are presented as the mean ± SEM. *$p < 0.05$, **$p < 0.01$, ***$p < 0.001$. See also Figure S1. BALF, bronchoalveolar lavage fluid; HE (Br), H&E-stained bronchia; HE (Ve), H&E-stained vessels.

apoptosis-related products in the lungs, although it did not fully halt their expression (Figures 2F and 2G, $p < 0.01$ or < 0.001). These results demonstrate that iPSC-MSC treatment alleviates allergic airway inflammation by restoring bronchial mitochondrial function and preventing apoptosis in the lungs.

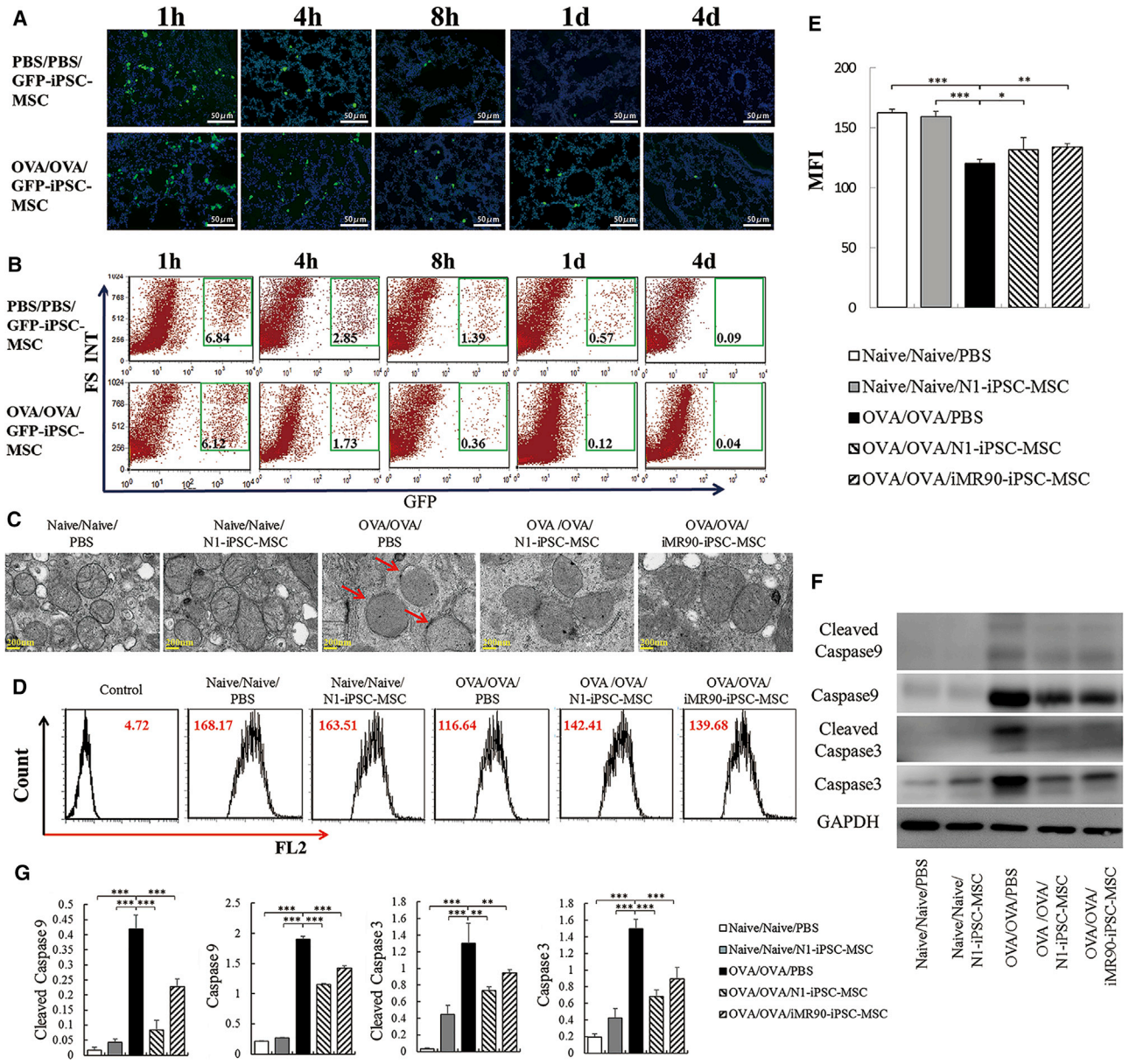

Figure 2. iPSC-MSC Treatment Reduces the Ultrastructural Changes and Mitochondrial Dysfunction in Injured Epithelial Cells

(A) Engraftment of iPSC-MSCs in the lungs at different time points (1 hr, 4 hr, 8 hr, 24 hr, 96 hr) after local transplantation was examined using iPSC-MSCs transfected with GFP (GFP-iPSC-MSCs, green).

(B) Flow cytometry analysis of the engraftment of GFP-iPSC-MSCs at different time points (1 hr, 4 hr, 8 hr, 24 hr, 96 hr). Experiments were carried out in triplicates.

(C) Representative TEM micrograph showing the morphological changes in the mitochondria of first-generation bronchi after iPSC-MSC treatment (the red arrow indicates the swollen mitochondria).

(D) Mitochondrial inner membrane potential for the mitochondria from lungs in each group was measured by flow cytometry.

(E) Statistical analysis of the mitochondrial inner membrane potential quantified by the mean fluorescence intensity in the FL2 channel (n = 6).

(F) Caspase 9 and caspase 3 activities related to apoptosis were measured in lung tissue from each group.

(G) Quantification of caspase 9, caspase 3, and their cleaved products in lung tissues from each group (n = 3).

Data are presented as the mean ± SEM. *p < 0.05, **p < 0.01, ***p < 0.001. BALF, bronchoalveolar lavage fluid; iPSC-MSCs, induced pluripotent stem cell-derived mesenchymal stem cells.

iPSC-MSCs Reduce $CoCl_2$-Induced Mitochondrial Dysfunction and Apoptosis in Epithelial Cells *In Vitro*

We examined the protective effects of iPSC-MSCs on epithelial cell mitochondrial dysfunction and apoptosis using the human BEAS-2B bronchial epithelium cell line. $CoCl_2$, a hypoxia mimic that can induce the transcription of hypoxia-inducible factor target genes and cause hypoxic injury and dysfunction in epithelial cells, was used to treat BEAS-2B cells; $CoCl_2$ (400 μM) was added to the culture medium for 12 hr to induce cellular apoptosis and impair the mitochondrial membrane potential. To test whether the protective effects of iPSC-MSCs were due to mitochondrial transfer to BEAS-2B cells via TNTs, non-specific potent actin polymerase inhibitors (cytochalasin D) and a connexin mimetic peptide (Gap26) were used. Administration of cytochalasin D and Gap26 did not affect iPSC-MSC viability (data not shown). BEAS-2B cells co-cultured with iPSC-MSCs exhibited significantly lower levels of apoptosis (Figures 3A and 3C, $p < 0.001$) and mitochondrial membrane potential in response to $CoCl_2$ (Figures 3B and 3D, $p < 0.001$) than BEAS-2B cells cultured without iPSC-MSCs. However, these protective effects of iPSC-MSCs were partially abrogated by cytochalasin D and Gap26 (Figures 3A–3D). Similarly, co-culture with iPSC-MSCs greatly reduced the reactive oxygen species (ROS) levels in BEAS-2B cells induced by $CoCl_2$. Gap26 treatment reversed these protective effects (Figures 3E and 3F, $p < 0.05$). Taken together, these results show that iPSC-MSCs protect against $CoCl_2$-induced mitochondrial dysfunction and apoptosis in BEAS-2B cells and that these protective effects may be due to mitochondrial function recovery via TNTs.

Mitochondrial Transfer from iPSC-MSCs to Epithelial Cells *In Vitro* and *In Vivo*

To investigate mitochondrial transfer from iPSC-MSCs to epithelial cells, we first examined the TNT formation between iPSC-MSCs and BEAS-2B cells. We found that clear TNT-like structures were formed between normal BEAS-2B cells (Figure 4A), between $CoCl_2$-treated BEAS-2B cells (Figure 4B), and between iPSC-MSCs (Figure 4C). Next, we treated BEAS-2B cells with or without $CoCl_2$ and then co-cultured them with iPSC-MSCs. Thin, tubular, and membranous-based structures ranging in size from 20 μm to 100 μm were clearly observed between both the iPSC-MSCs and BEAS-2B cells treated with and without $CoCl_2$ (Figures 4D and 4E). Time-lapse microscopy showed that the TNTs were involved in intercellular cytoplasmic component transportation and that the TNTs were originally formed by iPSC-MSCs. The number of TNTs from one iPSC-MSC was quantified under different conditions. More TNTs were formed between iPSC-MSCs and the damaged BEAS-2B cells than between the iPSC-MSCs and the normal BEAS-2B cells (Figure S2A). We next used MitoTracker Red to label mitochondria in iPSC-MSCs and 5(6)-carboxyfluorescein N-hydroxysuccinimidyl ester (CFSE) to label BEAS-2B cells (green) and then co-cultured the cells. iPSC-MSCs labeled with MitoTracker stretched out antennae and contacted the BEAS-2B cells labeled with CFSE (Figures S2B and S2C). Transfer of MitoTracker Red-labeled mitochondria from iPSC-MSCs to the CFSE-labeled BEAS-2B cells was observed at different time points (Figure 4F). Notably, mitochondrial transfer was detectable as early as 4 hr after co-culture, and the number of labeled mitochondria that were transferred into the BEAS-2B cells via TNTs increased over time (Figures 4F, S2B, and S2C).

To avoid potential MitoTracker leakage, we transfected iPSC-MSCs with Mitochondria-GFP (mGFP) and then co-cultured the cells with CellTrace Violet-labeled BEAS-2B cells (blue). This experiment revealed TNT formation between the iPSC-MSCs (Figure 5A) and the movement of green mitochondria from mGFP-iPSC-MSCs to $CoCl_2$-treated BEAS-2B cells (Figure 5B). GFP-positive mitochondria were clearly observed around the nuclei of BEAS-2B cells. In addition, flow cytometry analysis showed that the percentage of GFP-positive BEAS-2B cells was increased after 24 hr of co-culture and that up to 20% of BEAS-2B cells were positive for GFP after co-culture, suggesting that mitochondria were transferred from the mGFP-iPSC-MSCs to BEAS-2B cells (Figure 5C). Cytochalasin D and Gap26 treatment significantly reduced mitochondrial transfer from iPSC-MSCs to BEAS-2B cells, indicating that TNT plays a critical role in the regulation of mitochondrial transfer (Figure 5C). We next investigated whether engrafted iPSC-MSCs could donate mitochondria to bronchial epithelial cells in a mouse model of OVA-induced lung injury. The mGFP-iPSC-MSCs penetrated the OVA-induced lungs as quickly as 5 min after administration. GFP-labeled mitochondria started to appear in the lung cells at 1 hr post transplantation, and more mitochondria appeared in the lung tissue as time passed, even at 24 hr (Figure 5D). To determine whether the GFP-labeled mitochondria were located in alveolar epithelial cells, the alveolar epithelial cell-specific marker surfactant protein C (SPC) and the lung epithelial cell-specific marker Clara cell secretory protein (CCSP) were used to stain the epithelial cells at 24 hr after mGFP-iPSC-MSC administration. The staining revealed that the GFP-labeled mitochondria co-localized with both the alveolar epithelial and the bronchial cells (Figures 5E and 5F), demonstrating that the iPSC-MSCs donated their mitochondria to the epithelial cells of asthmatic mice. Taken together, these results suggest that iPSC-MSCs are capable of mitochondrial donation to injured epithelial cells via TNTs formed between these two cell types both *in vitro* and in mice.

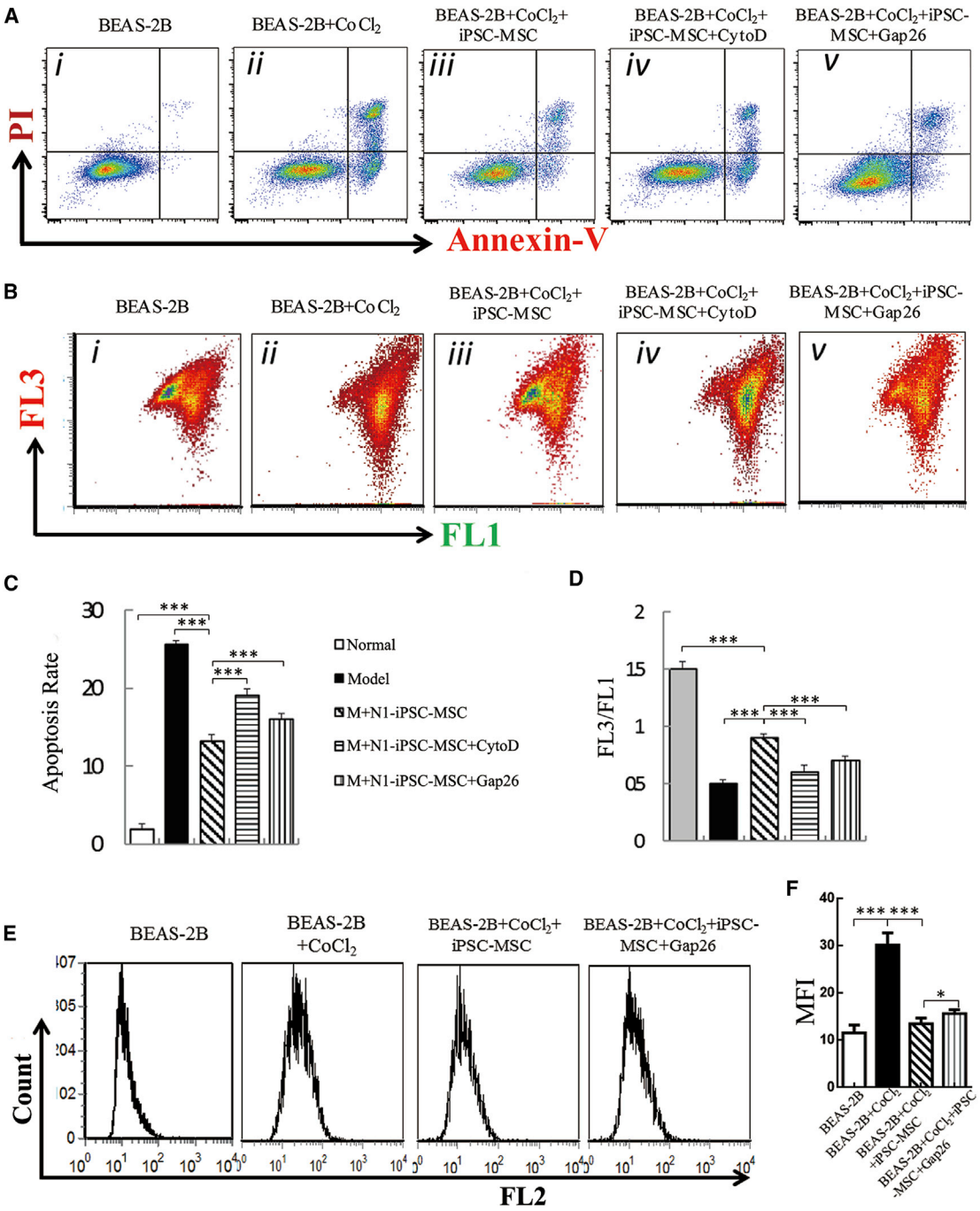

Figure 3. iPSC-MSCs Reduce $CoCl_2$-Induced Mitochondrial Dysfunction and Apoptosis in Epithelial Cells *In Vitro*

(A) Representative annexin V/propidium iodide (PI)-stained BEAS-2B cells analyzed by flow cytometry.

(B) Representative mitochondrial membrane potential measured by flow cytometry.

(C) Statistical analysis of the rate of BEAS-2B cell apoptosis (n = 6).

(D) Statistical analysis of the mitochondrial membrane potential in each group (n = 6).

(E) Representative reactive oxygen species in mitochondria (MitoROS) detected by flow cytometry.

(F) Statistical analysis of MitoROS in BEAS-2B cells (n = 6).

Data are presented as the mean ± SEM. *p < 0.05, ***p < 0.001. CytoD, cytochalasin D; iPSC-MSCs, induced pluripotent stem cell derived mesenchymal stem cells; PI, propidium iodide.

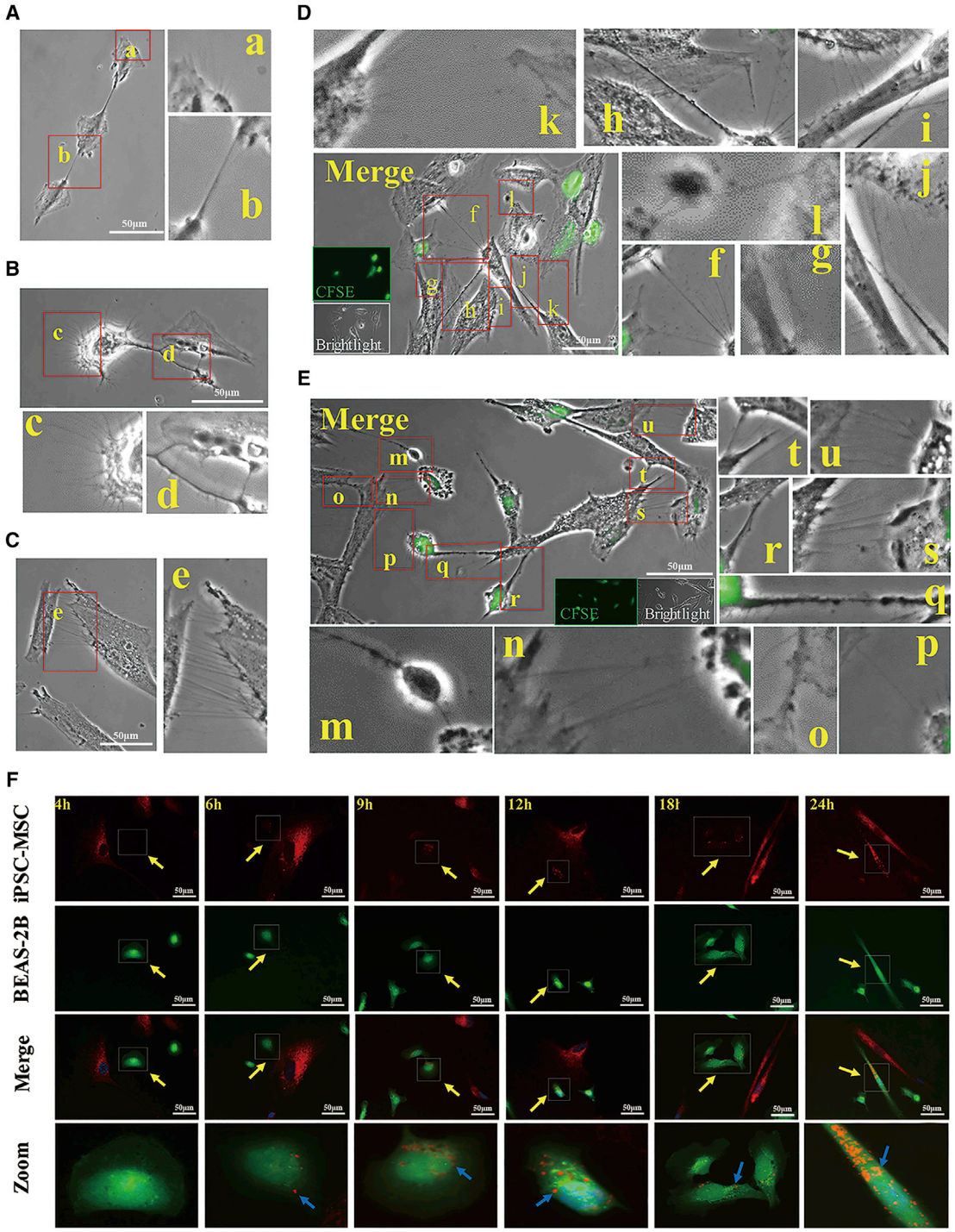

Figure 4. TNT Formation and Mitochondrial Transfer from iPSC-MSCs Labeled with MitoTracker into BEAS-2B Cells

(A–C) TNT-like structures were observed between normal BEAS-2B cells (A), between damaged BEAS-2B cells (B), and between normal iPSC-MSCs (C).

(D) TNTs were observed connecting iPSC-MSCs with normal BEAS-2B cells at 24 hr after co-culture.

(E) More TNTs were observed between iPSC-MSCs and $CoCl_2$-damaged BEAS-2B cells induced 24 hr after co-culture. TNTs were formed between normal BEAS-2B cells (b), damaged BEAS-2B cells (d), and normal N1-iPSC-MSCs (e); between normal N1-iPSC-MSCs and normal BEAS-2B cells (f, g, k); and between normal N1-iPSC-MSCs and damaged BEAS-2B cells (m, n, p, q, r, s, u).

(legend continued on next page)

CX43 Mediates the TNT Formation and Mitochondrial Transfer from iPSC-MSCs to Epithelial Cells and the Protective Ability of iPSC-MSCs against OVA-Induced Allergic Airway Inflammation

It has been reported that CX43 contributes to mitochondrial transfer from BM-MSCs to alveoli in acute lung injury (Islam et al., 2012). Therefore, we examined whether CX43 regulates the TNT formation and mitochondrial transfer from iPSC-MSCs to epithelial cells. We successfully overexpressed CX43 in the iPSC-MSCs by transfecting a CX43 plasmid (Figure S3A). We co-cultured iPSC-MSCs with BEAS-2B cells labeled with CellTrace Violet (blue). Immunostaining results showed weak expression of endogenous CX43 (red) in GFP-iPSC-MSCs, but CX43 expression was remarkably increased in the CX43-GFP-iPSC-MSCs (Figure 6A). Interestingly, positive CX43 staining was also observed in the TNTs between GFP-iPSC-MSCs and BEAS-2B cells (arrows, Figure 6A). Western blot analysis revealed similar expression of CX43 in the BEAS-2B cells and GFP-iPSC-MSCs and higher levels of expression in the CX43-GFP-iPSC-MSCs (Figure 6B, $p < 0.001$). CX43 was successfully silenced in the iPSC-MSCs using a plasmid expressing a short hairpin RNA against human CX43 (Figure S3B). We found that, in co-cultures with BEAS-2B cells, more TNTs extended from the CX43-GFP-iPSC-MSCs than from the shCX43-iPSC-MSCs and GFP-iPSC-MSCs (Figure 6C). Importantly, inhibition of CX43 by short hairpin RNA (shRNA) diminished the TNT formation in shCX43-iPSC-MSCs, indicating that CX43 directly or indirectly regulates TNT formation in iPSC-MSCs (Figure 6C). Flow cytometry analysis also revealed more GFP-positive BEAS-2B cells upon co-culture with CX43-GFP-iPSC-MSCs than with shCX43-iPSC-MSCs or controls, suggesting that more mitochondrial transfer events occurred in the CX43-GFP-iPSC-MSCs than in the shCX43-iPSC-MSCs (Figure 6D). Our findings suggested that CX43 played an important role in the regulation of TNT formation for the mitochondrial transfer between iPSC-MSCs and BEAS-2B cells.

Subsequently, CX43-GFP-iPSC-MSCs were transplanted into OVA-induced model mice to examine their effects on allergic airway inflammation. Compared with the GFP-iPSC-MSCs, the CX43-GFP-iPSC-MSCs demonstrated superior performance by alleviating inflammation and decreasing the mucus secretion of hyperplastic goblet cells in OVA-induced lungs (Figures 6E and 6F, $p < 0.05$). In addition, the levels of inflammatory cells in the BALF were decreased in the CX43-GFP-iPSC-MSC group compared with those in the GFP-iPSC-MSC group (Figure 6G, $p < 0.05$). Similarly, the Th2 cytokine (IL-4, IL-5, and IL-13) levels in the lavage fluid, the IgE levels in serum, and the epithelium-derived cytokines (IL-33 and TSLP) in lung homogenates were dramatically reduced in the CX43-GFP-iPSC-MSC group compared with those in the GFP-iPSC-MSC group (Figures 6H–6J, $p < 0.05$ or < 0.01). Compared with the iPSC-MSCs infected with a non-targeting control (Shcontrol [Sc]-iPSC-MSCs), the shCX43-iPSC-MSCs did not exhibit the immunomodulatory effects that prevent airway inflammation and mucus secretion as determined by the H&E inflammation score and mucus hypersecretion quantified by PAS in a mouse model of asthma (Figures 6E and 6F). Furthermore, the administration of shCX43-iPSC-MSCs resulted in higher levels of eosinophils, lymphocytes, neutrophils, and total inflammatory cells (Figure 6G, $p < 0.05$ or < 0.001); higher levels of IL-4, IL-5, and IL-13 in the BALF (Figure 6H, $p < 0.001$); higher serum levels of serum IgE and lower serum levels of IgG2a (Figure 6I, $p < 0.05$ or < 0.001); and higher levels of IL-33 and TSLP in the lung compared with those resulting from the administration of CX43-GFP-iPSC-MSCs (Figure 6J, $p < 0.001$). In summary, these results demonstrate that CX43 is critical for the mitochondrial transfer between iPSC-MSCs and epithelial cells during the attenuation of allergic airway inflammation.

We next examined whether CX43 is involved in the iPSC-MSC-mediated protection against OVA-induced mitochondrial dysfunction in allergic airway inflammation. Compared with that in the iPSC-MSC group, transfection with CX43 further restored mitochondrial inner membrane potential ($p < 0.05$), whereas the shCX43-iPSC-MSCs decreased this potential in OVA-induced mitochondrial dysfunction in the lung (Figures 7A and 7B). Furthermore, western blot analysis showed that overexpression of CX43 enhanced the iPSC-MSC-mediated inhibition of caspase 3 and caspase 9 expression as well as that of their cleaved products in lung tissue induced by OVA, whereas shCX43-iPSC-MSC treatment reversed these effects (Figures 7C and 7D).

Taken together, these findings demonstrate that overexpression of CX43 enhances the iPSC-MSC-mediated attenuation of allergic airway inflammation and rescue of mitochondrial dysfunction, whereas silencing CX43 in iPSC-MSCs partially abrogates these protective effects. These results suggest that CX43 is essential for TNT formation and iPSC-MSC-mediated mitochondrial transfer,

(F) iPSC-MSCs with MitoTracker Red-labeled mitochondria (red) were co-cultured with BEAS-2B cells (green). Mitochondrial transfer was detectable as early as 4 hr after co-culture. More mitochondria were transferred into BEAS-2B cells from iPSC-MSCs over time. BEAS-2B cells were labeled using CFSE (green) in (D)–(F). Experiments were carried out in triplicates.

CFSE, 5(6)-carboxyfluorescein N-hydroxysuccinimidyl ester; iPSC-MSC, induced pluripotent stem cell-derived mesenchymal stem cells; OVA, ovalbumin; TNT, tunneling nanotube. See also Figure S2.

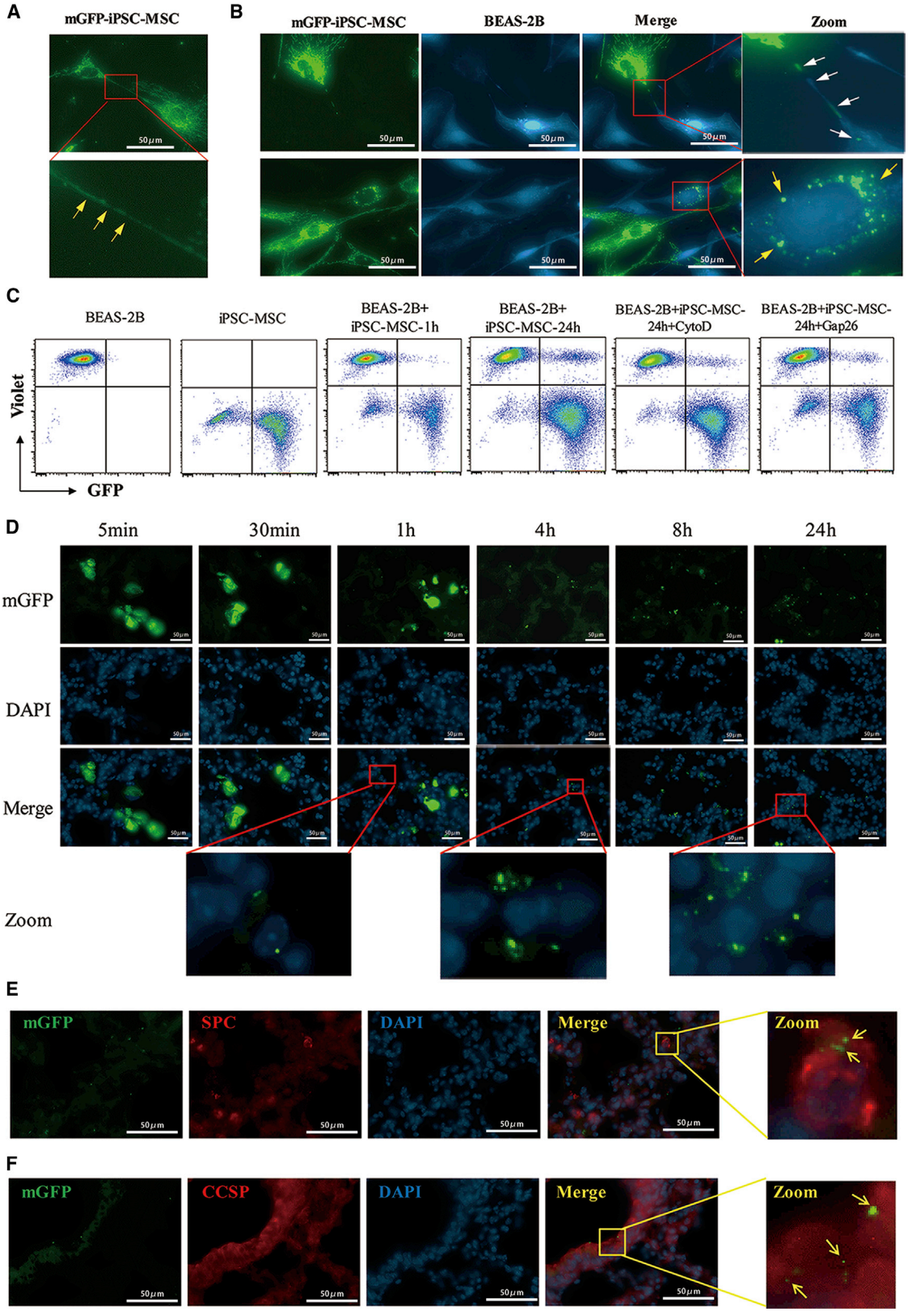

(legend on next page)

which alleviates the symptoms of allergic airway inflammation by restoring bronchial mitochondrial function and preventing apoptosis in the lungs.

DISCUSSION

MSC-based therapy has shown promising results for treating asthmatic inflammation by several mechanisms. This study focused on iPSC-MSC function in rescuing bronchial epithelial bioenergetics in asthma. We found that local transplantation of iPSC-MSCs alleviated asthma inflammation and protected the epithelial cells in mice via donating mitochondria to the dysfunctional mitochondrial epithelial cells. Mitochondria were transferred from iPSC-MSCs to epithelial cells via CX43-mediated TNTs, which bridged these two types of cells. The mitochondrial donation by iPSC-MSCs prevented the apoptosis of epithelial cells by restoring their mitochondrial function, alleviating the asthma inflammation caused by allergic or hypoxic conditions. Compared with MSCs isolated from BM and fetuses, we previously reported that iPSC-MSCs hold several advantages, including a higher proliferative capacity, higher differentiation potential, stronger immune privilege, and longer life span (Gao et al., 2017; Lian et al., 2010; Sun et al., 2015). The finding of this study is that CX43 contributes to mitochondrial transfer from iPSC-MSCs to epithelial cells via regulating TNT formation in asthma.

Epithelial cells mediate the innate and adaptive immune systems by releasing chemokines, cytokines, and alarmins (Hammad and Lambrecht, 2015). The airway epithelium is considered an essential controller of the inflammatory, immune, and regenerative responses to the allergens, viruses, and environmental pollutants that contribute to asthma pathogenesis (Lambrecht and Hammad, 2012). Increasing evidence shows that MSC transplantation can functionally ameliorate lung injury (de Castro et al., 2017; Takeda et al., 2018; Tilokee et al., 2016). Our previous studies demonstrated that intravenous injection of iPSC-MSCs inhibited allergic airway inflammation and permitted a rebalancing of the immune response in a mouse model (Sun et al., 2012; Wang et al., 2017). In this study, iPSC-MSCs were intratracheally injected into mice with OVA-induced asthma to investigate the effects of iPSC-MSCs on epithelial cells in asthma. Compared with that achieved with intravenous injection, the intratracheal injection of MSCs for the treatment of lung diseases may result in greater retention in the targeted tissue (Antunes et al., 2014; Bonios et al., 2011). We found that treatment with iPSC-MSCs dramatically reduced the expression of the epithelial cytokines IL-33 and TSLP and inhibited the apoptosis of BEAS-2B cells under $CoCl_2$ challenge, suggesting that local transplantation of iPSC-MSCs significantly inhibits asthma inflammation in the OVA-induced asthma mouse model.

Mitochondrial dysfunction in epithelial cells is reported responsible for allergic airway inflammation (Jaffer et al., 2015; Kim et al., 2014; Reddy, 2011). Treatment with mito-TEMPO, a mitochondrial-targeted antioxidant, inhibits OVA-induced allergic asthma in mice via attenuating mitochondrial ROS levels in epithelial cells (Jaffer et al., 2015). Therefore, targeting mitochondrial dysfunction may be an approach for allergic airway inflammation therapy. Previous studies have shown that MSCs can alleviate mitochondrial dysfunction in many cell types (Chuang et al., 2017; Li et al., 2018; Motegi et al., 2017). In the current study, administration of OVA led to swollen mitochondria and a decreased mitochondrial inner membrane potential in epithelial cells, indicating mitochondrial dysfunction. In contrast, transplantation of iPSC-MSCs greatly improved the mitochondrial morphology and partially restored the mitochondrial inner membrane potential. Furthermore,

Figure 5. Mitochondrial Transfer from mGFP-iPSC-MSCs into Epithelial Cells both *In Vitro* and in Mice

(A) Representative image of TNTs between iPSC-MSCs showing mGFP-labeled mitochondria (mGFP-iPSC-MSC, green).

(B) Representative image of mitochondria transferred from mGFP-iPSC-MSCs to damaged BEAS-2B cells induced by $CoCl_2$ (CellTrace Violet-labeled, blue). The white arrow shows green mitochondria moving from mGFP-iPSC-MSCs to damaged BEAS-2B cells. The circled, enlarged region, indicated by the yellow arrow, shows the accumulation of green mitochondria in one BEAS-2B cell.

(C) Mitochondrial transfer from mGFP-iPSC-MSCs to BEAS-2B cells was examined by fluorescence-activated cell sorting; cytochalasin D and Gap26 significantly suppressed the mitochondria transfer efficiency. Experiments were carried out in triplicates for (A)–(C).

(D) Representative images of iPSC-MSCs containing mGFP labeled mitochondria (mGFP-iPSC-MSC, green) in OVA-induced lungs at different time points after administration. The GFP expression in the pulmonary alveoli gradually increased after iPSC-MSC administration in OVA-induced mice (n = 3).

(E) Representative images for type II alveolar epithelial cells stained with SPC (alveolar epithelial cell-specific marker, red) and DAPI (nuclei, blue) at 24 hr; the enlarged region shows the presence of the GFP signal in SPC^+ cells.

(F) Representative images for bronchial epithelium stained with CCSP (lung epithelial cell-specific marker, red) and DAPI (nuclei, blue) at 24 hr; the enlarged region shows the presence of the GFP signal in $CCSP^+$ cells.

CCSP, Clara cell secretory protein; iPSC-MSC, induced pluripotent stem cell-derived mesenchymal stem cells; mGFP, mitochondrial targeting green fluorescence protein; SPC, surfactant protein C.

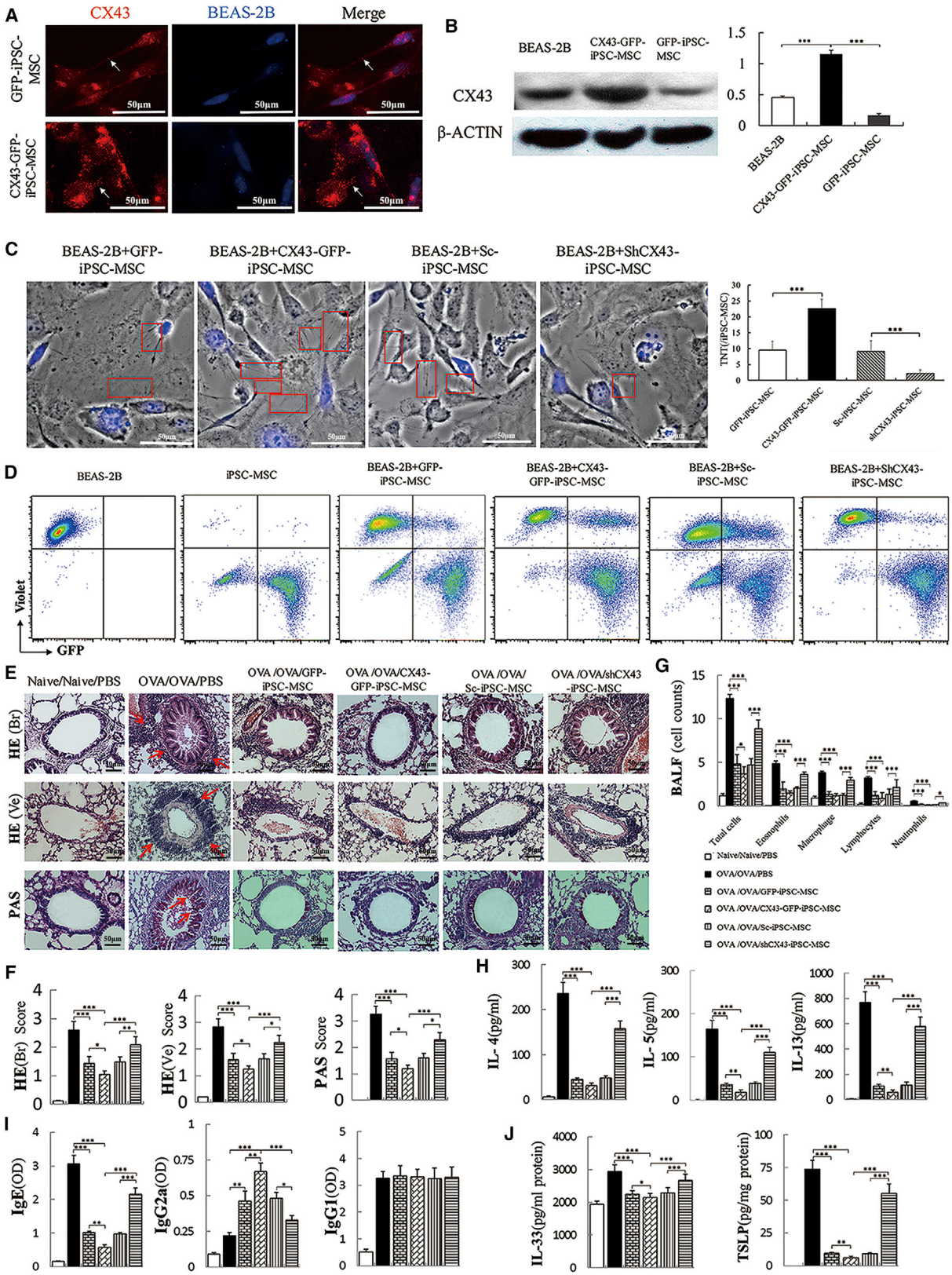

(legend on next page)

co-culture with iPSC-MSCs also reduced $CoCl_2$-induced mitochondrial dysfunction in epithelial cells, suggesting that the iPSC-MSC-mediated inhibition of asthma inflammation is due to the alleviation of mitochondrial dysfunction in epithelial cells. However, how iPSC-MSCs rescue mitochondrial dysfunction in epithelial cells remains largely unknown. Recent studies, including our own, have shown that MSCs can donate functional mitochondria to injured corneal epithelial cells and cardiomyocytes via TNT formation (Jiang et al., 2016; Phinney et al., 2015; Zhang et al., 2016). Here, we showed that iPSC-MSCs can donate mitochondria to epithelial cells with OVA- or $CoCl_2$-induced mitochondrial dysfunction via TNTs, which bridge iPSC-MSCs and injured epithelial cells and improve their mitochondrial function. Enhanced mitochondrial membrane potential may prevent cellular apoptotic processes, which could reduce allergic airway inflammation by preventing the release of pro-inflammatory factors (Cao et al., 2010; Gottlieb et al., 2003). These findings are in agreement with those of our previous studies showing that mitochondria transferred from iPSC-MSCs are functional and can inhibit cigarette smoke-induced lung injury and rescue anthracycline-induced cardiomyopathy (Li et al., 2014; Zhang et al., 2016). Furthermore, treatment with the TNT inhibitors significantly reduced the mitochondrial transfer efficiency from iPSC-MSCs to epithelial cells, indicating that TNT is essential for mitochondrial transfer.

Although there is considerable interest in investigating MSC mitochondrial transfer, the molecular regulators mediating mitochondrial transfer are not fully understood. Some molecular regulators that govern mitochondrial transfer have been identified. MIRO1 plays a critical role in regulating the mitochondrial transfer of MSCs, and overexpression of MIRO1 greatly enhances the mitochondrial transfer efficiency of iPSC-MSCs (Ahmad et al., 2014; Zhang et al., 2016). The microtubule motor protein kinesin family member 5B (KIF5B) has been considered to be a regulator of mitochondrial transfer (Shen et al., 2018). Islam et al. (2012) found that BM-MSCs donated mitochondria to alveolar progenitor cells via CX43 gap junctions in a mouse model of acute lung injury. In contrast, Sinclair et al. (2016) found that CX43 had no impact on the mitochondrial transfer of BM-MSCs. These contradictory findings may be due to the different sources of MSCs and the culture of MSCs under different conditions. There is increasing evidence for the existence of CX43 channels in TNTs, which could constitute a cellular strategy to regulate intercellular communication and contribute to the maintenance of homeostasis (He et al., 2011; Osswald et al., 2015; Ribeiro-Rodrigues et al., 2017). We found that CX43 is upregulated in mouse lungs during asthma (Yao et al., 2015). It has been reported that CX43 can stimulate TNT formation in HeLa cells (Lock et al., 2016). However, the pathophysiological implications of CX43-dependent channel activity in TNTs between iPSC-MSCs and epithelial cells remain to be clarified, and how CX43 behaves in the mitochondrial transfer of iPSC-MSCs in asthma-associated contexts is still unknown. To determine the role of CX43 in TNT formation and mitochondrial transfer between iPSC-MSCs and bronchial epithelial cells, genetic modification was employed to modify CX43 expression in iPSC-MSCs. These modifications demonstrated that, compared with iPSC-MSCs, overexpression of CX43 in iPSC-MSCs enhanced the TNT formation between iPSC-MSCs and epithelial cells *in vitro*, alleviated allergic airway inflammation, and significantly increased the mitochondrial transfer efficiency to epithelial cells, indicating that CX43 is a key regulator of TNT formation and mitochondrial transfer. Furthermore, silencing CX43 reduced TNF formation and the immunomodulatory effects of iPSC-MSCs during allergic airway inflammation.

Figure 6. CX43 Mediates the Mitochondrial Transfer from iPSC-MSCs to Epithelial Cells and the Protective Effect of iPSC-MSCs on OVA-Induced Allergic Airway Inflammation

(A) The representative expression of CX43 (red) in GFP-iPSC-MSCs and CX43-GFP-iPSC-MSCs upon co-culture with CellTrace Violet-labeled BEAS-2B cells (blue).

(B) Western blot analysis of CX43 expression in BEAS-2B cells, GFP-iPSC-MSCs, and CX43-GFP-iPSC-MSCs (n = 3).

(C) TNTs were observed connecting genetically modified iPSC-MSCs with $CoCl_2$-damaged BEAS-2B cells (blue) 24 hr after co-culture. More TNTs (red frame) were observed from CX43-GFP-iPSC-MSCs than from shCX43-iPSC-MSCs. Total of 30 iPSC-MSCs in five to six view fields were counted for TNT number (n = 3).

(D) Mitochondrial transfer from CX43-GFP-iPSC-MSCs and shCX43-iPSC-MSCs to BEAS-2B cells was determined by flow cytometry. Data are representative of three separate experiments.

(E) Representative images of H&E and PAS staining for inflammation and mucus accumulation in lungs, respectively.

(F) Statistical analysis of the inflammation score and mucus hypersecretion quantified by H&E/PAS scores (n = 6).

(G) Inflammatory cell counts in BALF (n = 6).

(H–J) The cytokine or Ig levels in BALF (H, n = 6), serum (I, n = 6) and lung homogenates (J, n = 6) as measured by ELISA.

Data are presented as the mean ± SEM. *$p < 0.05$, **$p < 0.01$, ***$p < 0.001$. See also Figure S3. BALF, bronchoalveolar lavage fluid; CX43, connexin 43; HE (Br), H&E-stained bronchia; HE (Ve), H&E-stained vessels; IL, interleukin; iPSC-MSC, induced pluripotent stem cell-derived mesenchymal stem cells; OVA, ovalbumin; PAS, periodic acid-Schiff; TSLP, thymic stromal lymphopoietin.

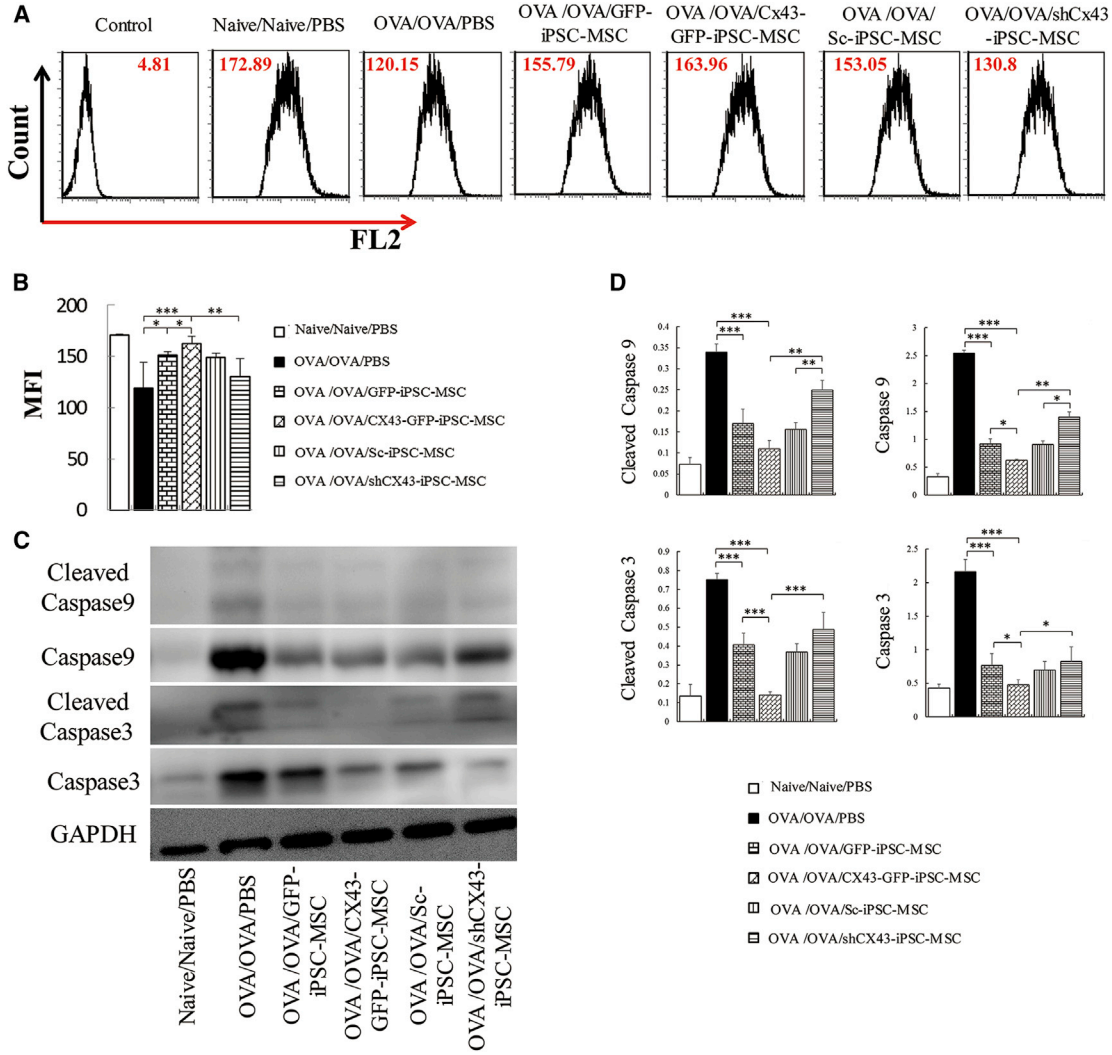

Figure 7. CX43 Mediates the Effects of iPSC-MSCs on Mitochondrial Dysfunction in a Mouse Model of Asthma

(A) Representative mitochondrial inner membrane potential measured by flow cytometry (n = 6).

(B) Statistical analysis of the mitochondrial inner membrane potential quantified by mean fluorescence intensity (n = 6).

(C) Western blot analysis of caspase 9 and caspase 3 activity.

(D) Quantification of caspase 9, caspase 3, and their cleaved products in lung tissues treated with genetically modified iPSC-MSCs (n = 3). Data are presented as the mean ± SEM. *p < 0.05, **p < 0.01, ***p < 0.001. BALF, bronchoalveolar lavage fluid; CX43, connexin 43; iPSC-MSC, induced pluripotent stem cell-derived mesenchymal stem cells; OVA, ovalbumin.

However, CX43 silencing did not completely prevent mitochondrial transfer from iPSC-MSCs to epithelial cells, indicating that other mechanisms are also involved in regulating mitochondrial transfer.

There are some limitations of this study. First, mitochondrial transfer is bidirectional, and whether the mitochondria in injured epithelial cells are transferred to iPSC-MSCs has not been elucidated. Second, although our results demonstrate that CX43 mediates the mitochondrial transfer efficacy of iPSC-MSCs, the signaling pathways involved in mitochondrial transfer have yet to be investigated. Detailed *in vivo* studies on the mitochondrial transfer from iPSC-MSCs to pulmonary alveoli in asthma require further investigation.

In conclusion, this study shows that, in addition to the immunomodulatory effect, the beneficial effect of iPSC-MSCs on allergic airway inflammation is in part due to mitochondrial transfer. Furthermore, CX43 is vital for regulating the TNT formation and mitochondrial transfer efficiency of iPSC-MSCs. Our study provides broader insight into the potential use of iPSC-MSCs as a treatment strategy for asthma.

EXPERIMENTAL PROCEDURES

Detailed descriptions of the methods are listed in the Supplemental Experimental Procedures.

Cell Culture

Two types of human iPSC-MSCs (N1-iPSC-MSCs and iMR90-iPSC-MSCs) were generated and cultured according to a previously described protocol (Lian et al., 2010). The human bronchial epithelium cell line (BEAS-2B cells) obtained from American Type Culture Collection (ATCC) was cultured in DMEM/F12 (HyClone, Logan, UT) supplemented with 10% FBS and 1% penicillin-streptomycin (Gibco, Carlsbad, CA) at 37°C, 5% CO_2, and 95% humidity.

Mouse Model of Asthma

All procedures involving animals were performed in accordance with the guidelines for animal experiments and approved by the Sun Yat-sen University Institutional Animal Care and Use Committee (approval no. 2013-61). The mouse model of OVA-induced asthma was modified according to our previous study (Sun et al., 2012), iPSC-MSCs were intratracheally delivered to the mice 24 hr prior to OVA challenge (Figure S4).

Histological Analysis of the Lungs

All the mice were sacrificed 6 hr after the last OVA challenge. H&E and PAS staining were performed to examine the inflammatory infiltrates and mucus accumulation.

Measurement of Inflammatory Cytokine and Ig Levels

BALF and serum were collected as previously described (Sun et al., 2012). The levels of various inflammatory cytokines (IL-4, IL-5 and IL-13 in BALF; IL-33 and TSLP in lung homogenate) as well as those of serum Ig (OVA-specific IgE, IgG1, and IgG2a) were measured.

Assessment of iPSC-MSC Engraftment

The engraftment of GFP-iPSC-MSCs in the lungs of mice at different time points (1 hr, 4 hr, 8 hr, 24 hr, and 96 hr) after local injection (n = 3) were examined by fluorescence microscopy (ZEISS LSM 800, Oberkochen, Germany) and flow cytometry (Beckman Coulter, Hercules, CA).

Assessment of Mitochondrial Inner Membrane Potential

BEAS-2B cells or mitochondria from lungs were incubated with the J-aggregate-forming lipophilic cation 5,5′,6,6′-tetrachloro-1,1′,3,3′-tetraethylbenzimidazolcarbocyanine iodide (JC-1, Sigma-Aldrich, St. Louis, MO) and then measured by flow cytometry.

Western Blot Analysis

Caspase 3 and caspase 9 levels in the lungs were detected with antibodies of caspase 3, cleaved caspase 3 (Asp175), caspase 9, and cleaved caspase 9 (Asp353) (Cell Signaling Technology, Beverly, MA) and the corresponding secondary antibodies (Santa Cruz Biotechnology, Dallas, TX) as previously described (Yao et al., 2015). The CX43 levels in the iPSC-MSCs were detected with an anti-CX43 antibody (BioLegend, San Diego, CA).

Overexpression and Silencing of CX43 in iPSC-MSCs

To determine whether CX43 is involved in the regulation of mitochondrial transfer of iPSC-MSCs, CX43-overexpressing iPSC-MSCs were prepared by lentiviral infection as previously described (Liang et al., 2015). CX43 in iPSC-MSCs was knocked down in iPSC-MSCs by shRNA (Vigene Biosciences, Rockville, MD). The genetically modified iPSC-MSCs were co-cultured with CellTrace Violet (Thermo Fisher Scientific, Boston, MA)-labeled BEAS-2B cells for validation before further transplantation.

Statistical Analysis

All experimental data are presented as the mean ± SEM. $p < 0.05$ was considered statistically significant.

SUPPLEMENTAL INFORMATION

Supplemental Information includes Supplemental Experimental Procedures and four figures and can be found with this article online at https://doi.org/10.1016/j.stemcr.2018.09.012.

AUTHOR CONTRIBUTIONS

Collection and/or assembly of data and data analysis, Y.Y.; Manuscript writing and data analysis, Y.Y., X.-L.F. and Y.Z.; Collection of data, X.L., Z.-B.X., and S.-B.F.; Preparation of iPSC-MSCs, D.J., S.C., H.-F.T., and Q.L.; Concept and design, manuscript writing, and final approval of the manuscript, Q.L. and Q.-L.F.

ACKNOWLEDGMENTS

This study was supported in part by grants from NSFC for Excellent Young Scholars (81322012 to Q.-L.F.), NSFC (81373174, 81471832, 81671882 and 81770984); the Hong Kong Research Grant Council General Research Fund (HKU17113816, HKU17120517 to Q.L.); NSFC (31571407 to Q.L.); the key grant from the Science and Technology Foundation of Guangdong Province of China (2015B020225001) and the Natural Science Foundation of Guangdong Province (2014A030313051, 2016A030308017, 2017A030313105).

Received: April 6, 2018
Revised: September 23, 2018
Accepted: September 24, 2018
Published: October 18, 2018

REFERENCES

Ahmad, T., Mukherjee, S., Pattnaik, B., Kumar, M., Singh, S., Kumar, M., Rehman, R., Tiwari, B.K., Jha, K.A., Barhanpurkar, A.P., et al. (2014). Miro1 regulates intercellular mitochondrial transport & enhances mesenchymal stem cell rescue efficacy. EMBO J. *33*, 994–1010.

Antunes, M.A., Abreu, S.C., Cruz, F.F., Teixeira, A.C., Lopes-Pacheco, M., Bandeira, E., Olsen, P.C., Diaz, B.L., Takyia, C.M., Freitas, I.P., et al. (2014). Effects of different mesenchymal stromal cell

sources and delivery routes in experimental emphysema. Respir. Res. *15*, 118.

Bonios, M., Terrovitis, J., Chang, C.Y., Engles, J.M., Higuchi, T., Lautamaki, R., Yu, J., Fox, J., Pomper, M., Wahl, R.L., et al. (2011). Myocardial substrate and route of administration determine acute cardiac retention and lung bio-distribution of cardiosphere-derived cells. J. Nucl. Cardiol. *18*, 443–450.

Cao, J., Wong, C.K., Yin, Y., and Lam, C.W. (2010). Activation of human bronchial epithelial cells by inflammatory cytokines IL-27 and TNF-alpha: implications for immunopathophysiology of airway inflammation. J. Cell Physiol. *223*, 788–797.

Chan, T.K., Tan, W.S.D., Peh, H.Y., and Wong, W.S.F. (2017). Aeroallergens induce reactive oxygen species production and DNA damage and dampen antioxidant responses in bronchial epithelial cells. J. Immunol. *199*, 39–47.

Chuang, Y.C., Liou, C.W., Chen, S.D., Wang, P.W., Chuang, J.H., Tiao, M.M., Hsu, T.Y., Lin, H.Y., and Lin, T.K. (2017). Mitochondrial transfer from Wharton's jelly mesenchymal stem cell to MERRF cybrid reduces oxidative stress and improves mitochondrial bioenergetics. Oxid. Med. Cell. Longev. *2017*, 5691215.

Crisostomo, P.R., Wang, M., Wairiuko, G.M., Morrell, E.D., Terrell, A.M., Seshadri, P., Nam, U.H., and Meldrum, D.R. (2006). High passage number of stem cells adversely affects stem cell activation and myocardial protection. Shock *26*, 575–580.

Cruz, F.F., Borg, Z.D., Goodwin, M., Sokocevic, D., Wagner, D.E., Coffey, A., Antunes, M., Robinson, K.L., Mitsialis, S.A., Kourembanas, S., et al. (2015). Systemic administration of human bone marrow-derived mesenchymal stromal cell extracellular vesicles ameliorates *Aspergillus* hyphal extract-induced allergic airway inflammation in immunocompetent mice. Stem Cells Transl. Med. *4*, 1302–1316.

Dai, R., Liu, J., Cai, S., Zheng, C., and Zhou, X. (2017). Delivery of adipose-derived mesenchymal stem cells attenuates airway responsiveness and inflammation in a mouse model of ovalbumin-induced asthma. Am. J. Transl. Res. *9*, 2421–2428.

de Castro, L.L., Xisto, D.G., Kitoko, J.Z., Cruz, F.F., Olsen, P.C., Redondo, P.A.G., Ferreira, T.P.T., Weiss, D.J., Martins, M.A., Morales, M.M., et al. (2017). Human adipose tissue mesenchymal stromal cells and their extracellular vesicles act differentially on lung mechanics and inflammation in experimental allergic asthma. Stem Cell Res. Ther. *8*, 151.

Fu, Q.L., Chow, Y.Y., Sun, S.J., Zeng, Q.X., Li, H.B., Shi, J.B., Sun, Y.Q., Wen, W., Tse, H.F., Lian, Q., et al. (2012). Mesenchymal stem cells derived from human induced pluripotent stem cells modulate T-cell phenotypes in allergic rhinitis. Allergy *67*, 1215–1222.

Gao, W.X., Sun, Y.Q., Shi, J., Li, C.L., Fang, S.B., Wang, D., Deng, X.Q., Wen, W., and Fu, Q.L. (2017). Effects of mesenchymal stem cells from human induced pluripotent stem cells on differentiation, maturation, and function of dendritic cells. Stem Cell Res. Ther. *8*, 48.

Gottlieb, E., Armour, S.M., Harris, M.H., and Thompson, C.B. (2003). Mitochondrial membrane potential regulates matrix configuration and cytochrome c release during apoptosis. Cell Death Differ. *10*, 709–717.

Hammad, H., and Lambrecht, B.N. (2015). Barrier epithelial cells and the control of type 2 immunity. Immunity *43*, 29–40.

He, K.M., Shi, X.L., Zhang, X.J., Dang, S., Ma, X.W., Liu, F., Xu, M., Lv, Z.Z., Han, D., Fang, X.H., et al. (2011). Long-distance intercellular connectivity between cardiomyocytes and cardiofibroblasts mediated by membrane nanotubes. Cardiovasc. Res. *92*, 39–47.

Islam, M.N., Das, S.R., Emin, M.T., Wei, M., Sun, L., Westphalen, K., Rowlands, D.J., Quadri, S.K., Bhattacharya, S., and Bhattacharya, J. (2012). Mitochondrial transfer from bone-marrow-derived stromal cells to pulmonary alveoli protects against acute lung injury. Nat. Med. *18*, 759–765.

Jaffer, O.A., Carter, A.B., Sanders, P.N., Dibbern, M.E., Winters, C.J., Murthy, S., Ryan, A.J., Rokita, A.G., Prasad, A.M., Zabner, J., et al. (2015). Mitochondrial-targeted antioxidant therapy decreases transforming growth factor-beta-mediated collagen production in a murine asthma model. Am. J. Respir. Cell Mol. Biol. *52*, 106–115.

Jiang, D., Gao, F., Zhang, Y., Wong, D.S., Li, Q., Tse, H.F., Xu, G., Yu, Z., and Lian, Q. (2016). Mitochondrial transfer of mesenchymal stem cells effectively protects corneal epithelial cells from mitochondrial damage. Cell Death Dis. *7*, e2467.

Kim, S.R., Kim, D.I., Kim, S.H., Lee, H., Lee, K.S., Cho, S.H., and Lee, Y.C. (2014). NLRP3 inflammasome activation by mitochondrial ROS in bronchial epithelial cells is required for allergic inflammation. Cell Death Dis. *5*, e1498.

Lambrecht, B.N., and Hammad, H. (2012). The airway epithelium in asthma. Nat. Med. *18*, 684–692.

Lambrecht, B.N., and Hammad, H. (2015). The immunology of asthma. Nat. Immunol. *16*, 45–56.

Li, X., Zhang, Y., Yeung, S.C., Liang, Y., Liang, X., Ding, Y., Ip, M.S., Tse, H.F., Mak, J.C., and Lian, Q. (2014). Mitochondrial transfer of induced pluripotent stem cell-derived mesenchymal stem cells to airway epithelial cells attenuates cigarette smoke-induced damage. Am. J. Respir. Cell Mol. Biol. *51*, 455–465.

Li, X., Michaeloudes, C., Zhang, Y., Wiegman, C.H., Adcock, I.M., Lian, Q., Mak, J.C.W., Bhavsar, P.K., and Chung, K.F. (2018). Mesenchymal stem cells alleviate oxidative stress-induced mitochondrial dysfunction in the airways. J. Allergy Clin. Immunol. *141*, 1634–1645.e5.

Lian, Q., Zhang, Y., Zhang, J., Zhang, H.K., Wu, X., Zhang, Y., Lam, F.F., Kang, S., Xia, J.C., Lai, W.H., et al. (2010). Functional mesenchymal stem cells derived from human induced pluripotent stem cells attenuate limb ischemia in mice. Circulation *121*, 1113–1123.

Liang, X., Ding, Y., Zhang, Y., Chai, Y.H., He, J., Chiu, S.M., Gao, F., Tse, H.F., and Lian, Q. (2015). Activation of NRG1-ERBB4 signaling potentiates mesenchymal stem cell-mediated myocardial repairs following myocardial infarction. Cell Death Dis. *6*, e1765.

Lock, J.T., Parker, I., and Smith, I.F. (2016). Communication of Ca(2+) signals via tunneling membrane nanotubes is mediated by transmission of inositol trisphosphate through gap junctions. Cell Calcium *60*, 266–272.

Motegi, S.I., Sekiguchi, A., Uchiyama, A., Uehara, A., Fujiwara, C., Yamazaki, S., Perera, B., Nakamura, H., Ogino, S., Yokoyama, Y., et al. (2017). Protective effect of mesenchymal stem cells on the pressure ulcer formation by the regulation of oxidative and endoplasmic reticulum stress. Sci. Rep. *7*, 17186.

Osswald, M., Jung, E., Sahm, F., Solecki, G., Venkataramani, V., Blaes, J., Weil, S., Horstmann, H., Wiestler, B., Syed, M., et al. (2015). Brain tumour cells interconnect to a functional and resistant network. Nature *528*, 93–98.

Phinney, D.G., Di Giuseppe, M., Njah, J., Sala, E., Shiva, S., St Croix, C.M., Stolz, D.B., Watkins, S.C., Di, Y.P., Leikauf, G.D., et al. (2015). Mesenchymal stem cells use extracellular vesicles to outsource mitophagy and shuttle microRNAs. Nat. Commun. *6*, 8472.

Plotkowski, M.C., Povoa, H.C., Zahm, J.M., Lizard, G., Pereira, G.M., Tournier, J.M., and Puchelle, E. (2002). Early mitochondrial dysfunction, superoxide anion production, and DNA degradation are associated with non-apoptotic death of human airway epithelial cells induced by *Pseudomonas aeruginosa* exotoxin A. Am. J. Respir. Cell Mol. Biol. *26*, 617–626.

Poole, J.A. (2014). Asthma is a major noncommunicable disease affecting over 230 million people worldwide and represents the most common chronic disease among children. Int. Immunopharmacol. *23*, 315.

Reddy, P.H. (2011). Mitochondrial dysfunction and oxidative stress in asthma: implications for mitochondria-targeted antioxidant therapeutics. Pharmaceuticals (Basel) *4*, 429–456.

Ribeiro-Rodrigues, T.M., Martins-Marques, T., Morel, S., Kwak, B.R., and Girao, H. (2017). Role of connexin 43 in different forms of intercellular communication - gap junctions, extracellular vesicles and tunnelling nanotubes. J. Cell Sci. *130*, 3619–3630.

Shen, J., Zhang, J.H., Xiao, H., Wu, J.M., He, K.M., Lv, Z.Z., Li, Z.J., Xu, M., and Zhang, Y.Y. (2018). Mitochondria are transported along microtubules in membrane nanotubes to rescue distressed cardiomyocytes from apoptosis. Cell Death Dis. *9*, 81.

Sinclair, K.A., Yerkovich, S.T., Hopkins, P.M., and Chambers, D.C. (2016). Characterization of intercellular communication and mitochondrial donation by mesenchymal stromal cells derived from the human lung. Stem Cell Res. Ther. *7*, 91.

Spees, J.L., Olson, S.D., Whitney, M.J., and Prockop, D.J. (2006). Mitochondrial transfer between cells can rescue aerobic respiration. Proc. Natl. Acad. Sci. U S A *103*, 1283–1288.

Sun, Y.Q., Deng, M.X., He, J., Zeng, Q.X., Wen, W., Wong, D.S., Tse, H.F., Xu, G., Lian, Q., Shi, J., et al. (2012). Human pluripotent stem cell-derived mesenchymal stem cells prevent allergic airway inflammation in mice. Stem Cells *30*, 2692–2699.

Sun, Y.Q., Zhang, Y., Li, X., Deng, M.X., Gao, W.X., Yao, Y., Chiu, S.M., Liang, X., Gao, F., Chan, C.W., et al. (2015). Insensitivity of human iPS cells-derived mesenchymal stem cells to interferon-gamma-induced HLA expression potentiates repair efficiency of hind limb ischemia in immune humanized NOD scid gamma mice. Stem Cells *33*, 3452–3467.

Takeda, K., Webb, T.L., Ning, F., Shiraishi, Y., Regan, D.P., Chow, L., Smith, M.J., Ashino, S., Guth, A.M., Hopkins, S., et al. (2018). Mesenchymal stem cells recruit CCR2(+) monocytes to suppress allergic airway inflammation. J. Immunol. *200*, 1261–1269.

Tilokee, E.L., Latham, N., Jackson, R., Mayfield, A.E., Ye, B., Mount, S., Lam, B.K., Suuronen, E.J., Ruel, M., Stewart, D.J., et al. (2016). Paracrine engineering of human explant-derived cardiac stem cells to over-express stromal-cell derived factor 1alpha enhances myocardial repair. Stem Cells *34*, 1826–1835.

Wang, S.Y., Fan, X.L., Yu, Q.N., Deng, M.X., Sun, Y.Q., Gao, W.X., Li, C.L., Shi, J.B., and Fu, Q.L. (2017). The lncRNAs involved in mouse airway allergic inflammation following induced pluripotent stem cell-mesenchymal stem cell treatment. Stem Cell Res. Ther. *8*, 2.

Yao, Y., Zeng, Q.X., Deng, X.Q., Tang, G.N., Guo, J.B., Sun, Y.Q., Ru, K., Rizzo, A.N., Shi, J.B., and Fu, Q.L. (2015). Connexin 43 upregulation in mouse lungs during ovalbumin-induced asthma. PLoS One *10*, e0144106.

Zar, H.J., and Levin, M.E. (2012). Challenges in treating pediatric asthma in developing countries. Paediatr. Drugs *14*, 353–359.

Zhang, Y., Yu, Z., Jiang, D., Liang, X., Liao, S., Zhang, Z., Yue, W., Li, X., Chiu, S.M., Chai, Y.H., et al. (2016). iPSC-MSCs with high intrinsic MIRO1 and sensitivity to TNF-alpha yield efficacious mitochondrial transfer to rescue anthracycline-induced cardiomyopathy. Stem Cell Reports *7*, 749–763.

Stem Cell Reports, Volume *11*

Supplemental Information

Connexin 43-Mediated Mitochondrial Transfer of iPSC-MSCs Alleviates Asthma Inflammation

Yin Yao, Xing-Liang Fan, Dan Jiang, Yuelin Zhang, Xin Li, Zhi-Bin Xu, Shu-Bin Fang, Sinming Chiu, Hung-Fat Tse, Qizhou Lian, and Qing-Ling Fu

Supplemental Figures

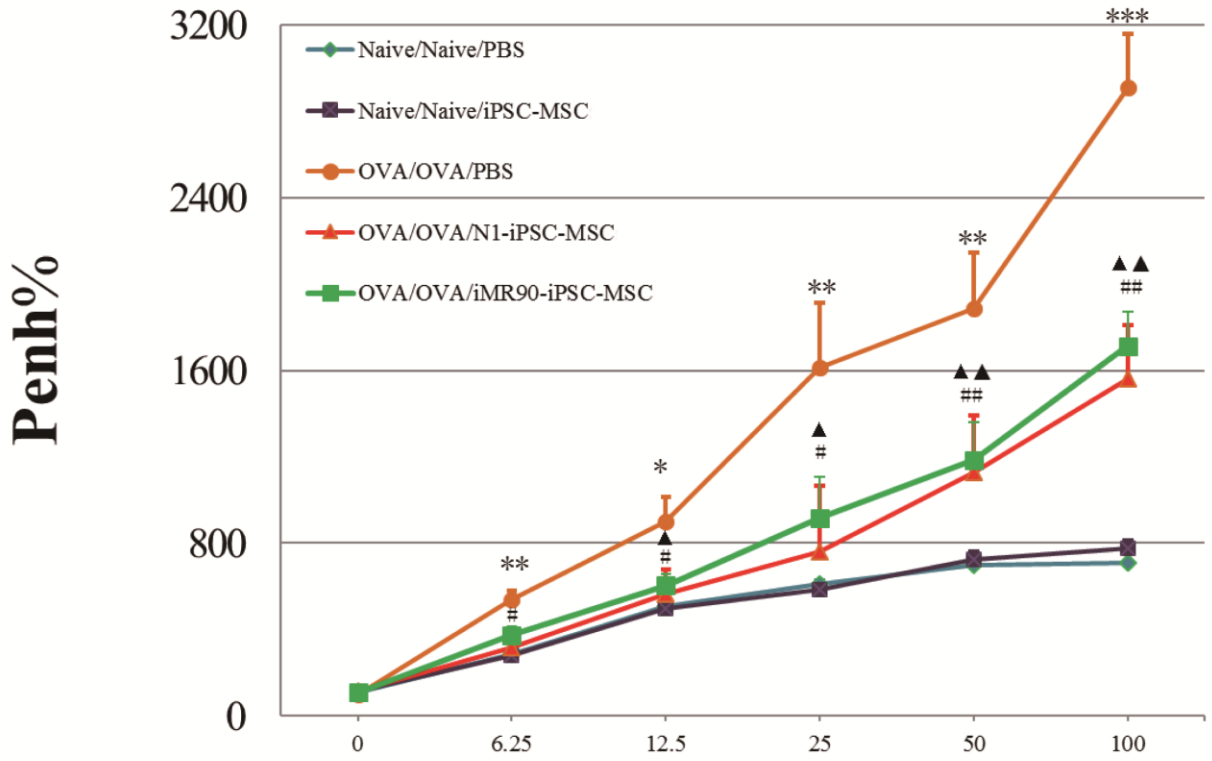

Figure S1. iPSC-MSCs alleviated mouse airway responsiveness. Related to Figure 1.
The OVA/OVA/PBS mice presented remarkably high airway to increased methacholine (Mch) dosages (6.25, 12.5, 25, 50 and 100 mg/ml) compared to control. iPSC-MSC treatment reduced the OVA-induced airway hyperresponsiveness in mice.
* for comparison between OVA/OVA/PBS and Naive/Naive/PBS; # for comparison between OVA/OVA/N1-iPSC-MSC and OVA/OVA/PBS; ▲ for comparison between OVA/OVA/iMR90-iPSC-MSC and OVA/OVA/PBS. Data are presented as the mean ± SEM. n = 6, *, # and ▲$p < 0.05$, **, ## and ▲▲$p < 0.01$, ***$p < 0.001$.
Abbreviations: iPSC-MSCs, induced pluripotent stem cell derived mesenchymal stem cells; OVA, ovalbumin.

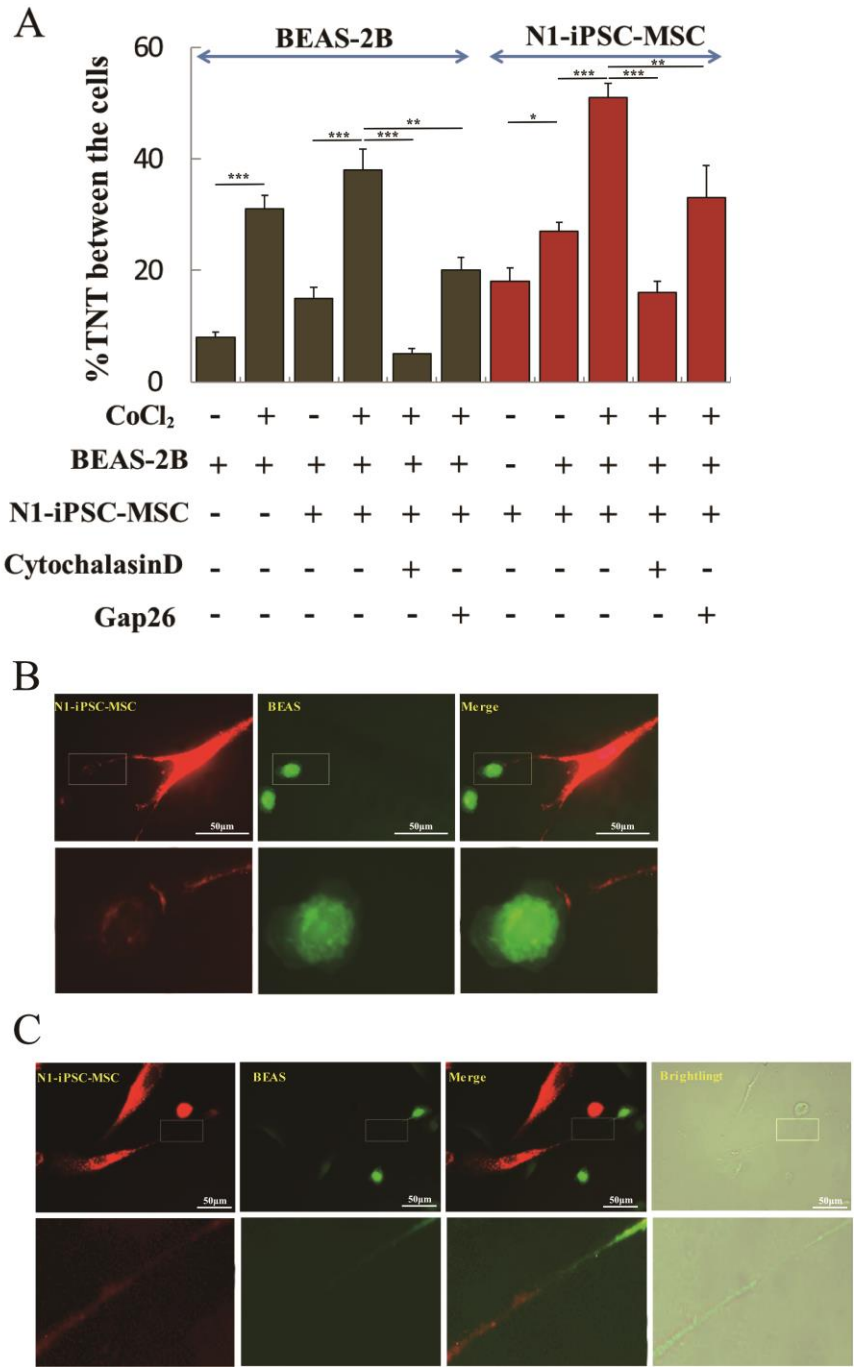

Figure S2. The TNT formation between N1-iPSC-MSCs and $CoCl_2$ damaged BEAS-2B cells *in vitro*. Related to Figure 4.

(A) The percentage of TNT formed cells was quantified in BEAS-2B cells or iPSC-MSCs (n = 3). Data are presented as the mean ± SEM.

(B) iPSC-MSCs stretched out the antennae and touched the BEAS-2B cells 4 h after co-culture.

(C) TNTs between iPSC-MSCs and BEAS-2B cells were detected 24 h after co-culture.

Cytochalasin D: non-specificity potent actin polymerase inhibitors; Gap26: CX43 peptides gap 26.

Abbreviations: CX43, connexin 43; iPSC-MSCs, induced pluripotent stem cell derived mesenchymal stem cells; TNT, tunnelling nanotube.

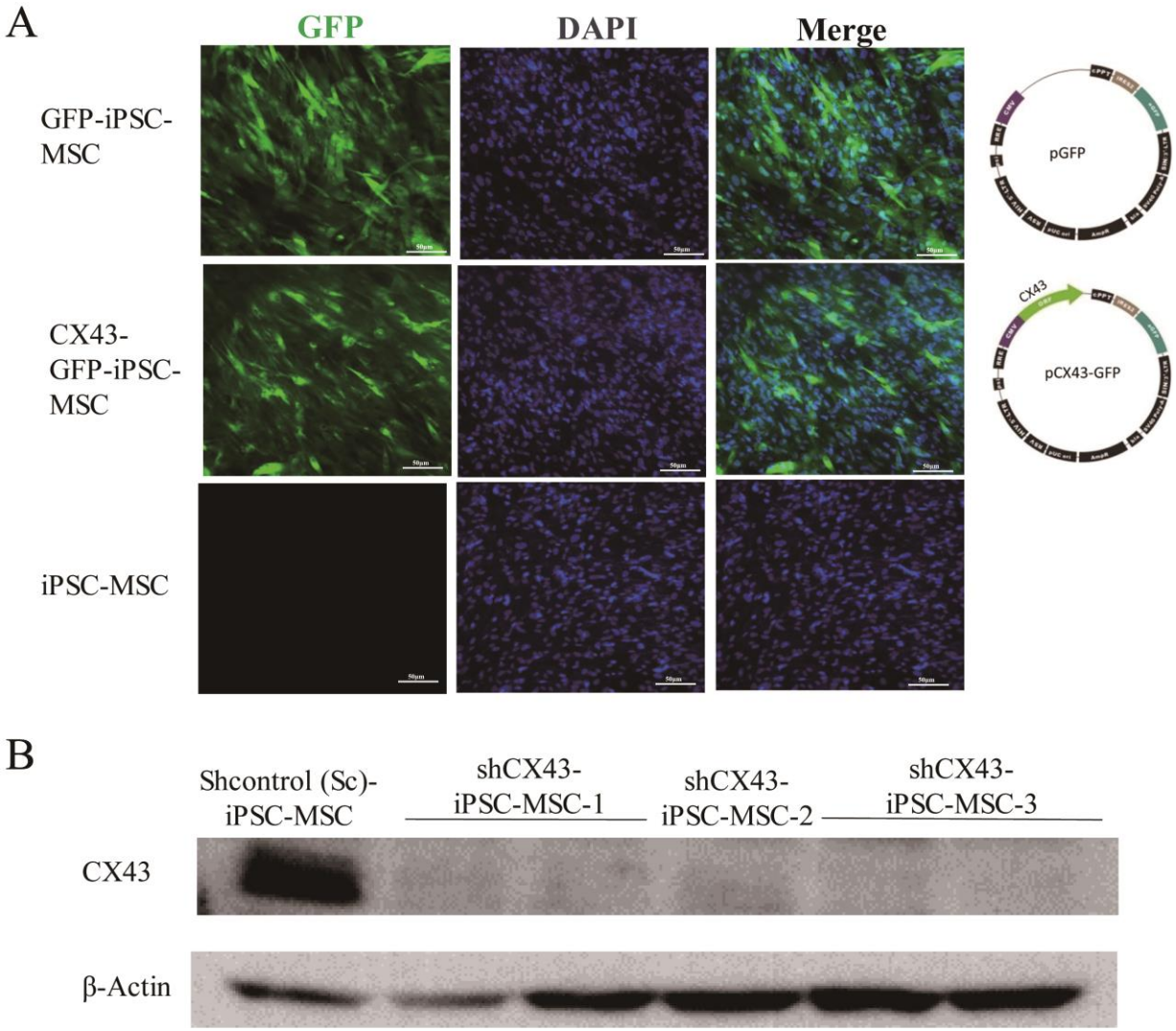

Figure S3. CX43 overexpression and silencing in iPSC-MSCs. Related to Figure 6.
(A) pCX43-GFP and control pGFP lentivirus based recombinant plasmids were constructed and then transfected into iPSC-MSCs using lentiviral packaging system. Immunofluorescence examination showed strong GFP signals in the transfected cells, which demonstrated good transfection efficiency.
(B) Western blot analysis of CX43 expression after shRNA knockdown, which expression was significantly decreased by the synthetic shRNA.
Abbreviations: CX43, connexin 43; iPSC-MSCs, induced pluripotent stem cell derived mesenchymal stem cells.

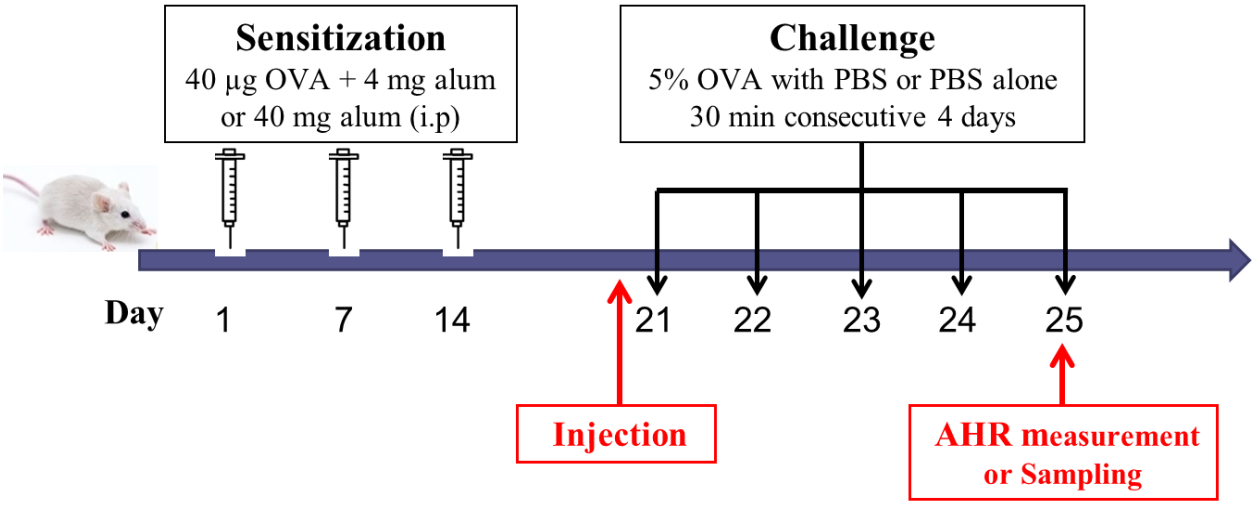

Figure S4. The procedure of OVA-induction asthma model and iPSC-MSC treatment. Related to the 'Mouse model of asthma' section.

For sensitization, the mice received an i.p injection of OVA or PBS with aluminium hydroxide on day 1, day 7 and day 14. From day 21 to 25, the mice were challenged with aerosolized 5% OVA or PBS in a plexiglass chamber for 30 minutes each day. A total of 5×10^5 iPSC-MSCs in 50 µl PBS was injected via trachea before challenge. Samples were collected on day 25.

Abbreviations: i.p, intraperitoneal; OVA, ovalbumin; PBS, phosphate-buffered saline.

Supplemental Experimental Procedures

iPSC-MSC culture

Briefly, iPSC-MSCs were positive for CD105, CD73, CD90, CD146, CD144, and CD44, but negative for CD34, CD14, and CD45. Their osteogenic, chondrogenic and adipogenic differentiation capacity of iPSC-MSCs were also confirmed (Lian et al., 2010). The generated iPSC-MSCs were cultured in Dulbecco's modified Eagle medium (DMEM, Gibco, Carlsbad, CA) supplemented with 15% fetal bovine serum (FBS, Gibco, Carlsbad, CA), 1% penicillin-streptomycin (Gibco, Carlsbad, CA), 5 ng/ml EGF (PeproTech, Rocky Hill, NJ) and 5 ng/ml β-FGF (PeproTech, Rocky Hill, NJ) at 37℃, 5% CO_2 and 95% humidity. iPSC-MSCs in passage 8-12 were used in this study.

Mouse model of asthma

Female BALB/c mice (4~6 weeks of age) were purchased from the Guangdong Medical Laboratory Animal Centre (Guangzhou, China). Briefly, the mice were sensitized with 40 μg Ovalbumin (OVA) or phosphate-buffered saline (PBS) with 100 μl Inject Alum (Thermo Fisher Scientific, Boston, MA) at day 1, day 7 and day 14 via an intraperitoneal (ip.) injection, respectively. From day 21 to 25, the mice were challenged with aerosolized 5% OVA or PBS for 30 minutes/day. A total of 5×10^5 iPSC-MSCs in 50 μl PBS were intratracheally injected into mice. The mice were randomly divided into different groups: (1) Naive/Naive/PBS mice were naive mice injected with PBS on day 20; (2) naive/naive/ iPSC-MSCs mice that were naive mice treated with iPSC-MSCs on day 20; (3) OVA/OVA/PBS mice that were sensitized and challenged with OVA, then treated with PBS on day 20; (4) OVA/OVA/ iPSC-MSCs mice that were sensitized and challenged with OVA and then treated with iPSC-MSCs on day 20. A brief illustration of the mouse model establishment was listed in Figure S4. Airway hyperresponsiveness (AHR) to methacholine (Mch) was measured to confirm the asthmatic inflammation 24 h after the last challenge as previously described (Yao et al., 2015). The mice were sacrificed at 6 h after the last challenge and the lungs were harvested for histological examination. The mitochondrial morphology in the epithelial cells was analyzed by TEM scanning.

Histological examination of the lungs

The mice were sacrificed at 6 h after the last challenge. The inferior lobes of the left lung were were harvested, fixed in 4% formalin overnight, embedded in paraffin and sectioned. Hematoxylin-eosin (HE) and periodic acid–schiff (PAS, Baso Diagnostics Inc., Zhuhai, China) staining was performed to assess the degree of airway inflammation. For a quantification of lung inflammation, the goblet cell counts and inflammatory infiltration scores in the lungs were performed as previously described (Yao et al., 2015).

Measurement of inflammatory cytokine and immunoglobulin (Ig) levels

Six hours after the last challenge, bronchoalveolar lavage fluid (BALF) and serum were collected (Sun et al., 2012). The collected BALF and serum were centrifuged at 700 g for 8 min at 4℃. After centrifugation, the types of cells including eosinophils, macrophages, neutrophils, and lymphocytes presented within the BALF were counted with Diff-Quick method (Baso Diagnostics Inc.). The levels of IL-4, IL-5 and IL-13 in the supernatants of BALF, and the levels of IL-33 and thymic stromal lymphopoietin (TSLP) in the lung homogenate were measured by sandwich enzyme-linked immuno sorbent assay (ELISA) analysis following the manufacturer’s instructions

(R&D Systems, Minneapolis, MN). OVA-specific IgE, IgG1 and IgG2a in the serum were measured as previously described (Yao et al., 2015).

Assessment of iPSC-MSC engraftment

Fluorescent microscopy and flow cytometry analysis were used to detect the engraftment of GFP transfected iPSC-MSCs (GFP-iPSC-MSCs) in the lungs of mouse models at different time points (1 h, 4 h, 8 h, 24 h, and 96 h) after local injection on day 20 (n = 3). For GFP transfection, the cells were nucleofected with the GFP reporter gene as previously described (Aslan et al., 2006; Sheyn et al., 2016; Sheyn et al., 2011), and the transfected cells were sorted by flow cytometry. For fluorescent microscopy, the lungs were cryosectioned and counterstained with 5 μg/ml 4', 6'-diamidino-2-phenylindole (DAPI) (Biyuntian, Inc., Shanghai, China) to identify cellular nuclei. The images were captured using a confocal fluorescence microscope. For flow cytometry analysis, the lungs were isolated and enzymatically digested using dispase (BD Biosciences, San Jose, CA) combined collagenases I (Sigma-Aldrich, St. Louis, MO). A 70 μm mesh was used to filter the mixed lung cells to obtain single-cell suspensions for analysis. The percentage of GFP^+ cells (GFP-iPSC-MSCs) were counted and analysed using FlowJo software (Tree Star, Inc., Ashland, Oregon).

Assessment of mitochondrial inner membrane potential

Mitochondria from lungs were isolated using an Isolated Mitochondria Staining Kit (Sigma-Aldrich, St. Louis, MO) and incubated with the sensitive fluorescent probe J-aggregate-forming lipophilic cation 5,5',6,6'-tetrachloro-1,1',3,3'-tetraethylbenzimidazolcarbocyanine iodide (JC-1, 0.5 mg/ml, Sigma-Aldrich, St. Louis, MO) and then measured by flow cytometry. The results were expressed as the mean fluorescence intensity in FL2 channel.

Mitochondria from BEAS-2B cells were stained with JC-1 at 37°C for 15 min and then measured by flow cytometry. The results were expressed as the mean fluorescence intensity in FL3 channel to that in FL1 channel.

Western blot analysis

To measure the mitochondria-related Caspase 3 and Caspase 9 levels, the lungs were dissected and homogenized in lysis buffer (10 mM Tris, pH 7.4, 150 mM NaCl, 1 mMEDTA, and 1 mMEGTA) supplemented with 1% protease inhibitor and 1% phosphatase inhibitor cocktails (Sigma-Aldrich, St. Louis, MO). After transferred to PVDF membranes, Caspase-3 Antibody, Cleaved Caspase-3 (Asp175) Antibody, Caspase-9 Antibody, Cleaved Caspase-9 (Asp353) Antibody (Cell Signaling Technology, Beverly, MA) and corresponding secondary antibodies (Santa Cruz Biotechnology, Dallas,TX) were used to detect the mitochondria-related Caspase 3 and Caspase 9 levels. Protein loading was controlled for normalization using a monoclonal mouse antibody against anti-GAPDH (Abcam, Cambridge, UK). The intensity of each band was quantified using ImageJ software. All western blot experiments were performed in triplicate.

Mitochondrial transfer from iPSC-MSCs to epithelial cells

As our previous study (Zhang et al., 2016), 2×10^5 iPSC-MSCs were cultured one day before transfection and then lentiviral-mediated mitochondrial targeting green fluorescence protein (pCT-MITO-GFP, Cat: Cyto102-PA-1, System Biosciences, Palo Alto, CA) was added to 1 ml growth medium with polybrene transfection reagent (TR-1003-G, Merck Millipore, Billerica, MA). The transfected iPSC-MSCs (mGFP-iPSC-MSCs) were cultured for 16 h. mGFP-iPSC-MSCs were administrated into the OVA-induced mice on day 20. The GFP expression levels in the pulmonary

alveoli were examined at different time points (5 min, 30 min, 1 h, 4 h, 8 h, and 24 h) post administration. To examine the mitochondrial transfer from iPSC-MSCs to the epithelial cells, the alveolar epithelial cells and bronchial epithelium were incubated with surfactant protein C (SPC) and clara cell secretory protein (CCSP) primary antibodies and AlexaFluor 568 secondary antibody 24 h after the administration.

In addition, the MitoTracker® Red CMXRos (Thermo Fisher Scientific, Boston, MA) labelled iPSC-MSCs were co-cultured with CFSE (Thermo Fisher Scientific, Boston, MA) labelled BEAS-2B cells *in vitro*. After 24 h co-culture, the tunneling nanotube (TNT) formation between iPSC-MSCs and BEAS-2B and the mitochondrial transfer were examined under fluorescent microscope (IX81-ZDC2, Olympus). Cytochalasin D (actin polymerase inhibitor, 100 nM, Sigma-Aldrich, St. Louis, MO) and Gap26 (connexin mimetic peptide, 0.25 mg/ml, APExBIO, Boston, MA) were added into the co-culture system to inhibit the TNT formation. The percentage of TNTs formed in BEAS-2B cells or iPSC-MSCs were quantified. Flow cytometry was employed to identify the dead BEAS-2B and measure the mitochondrial membrane potential as well as reactive oxygen species (ROS) in mitochondria (MitoSOX™ Red, 5 μM, Thermo Fisher Scientific, Boston, MA). The apoptosis rate was expressed as the Annexin-V positive cells. The MitoSOX was expressed as the mean fluorescence intensity in FL2.

For the determination of TNT formation, CX43-GFP-iPSC-MSCs, ShCX43-iPSC-MSCs and their control cells were co-cultured with CellTrace Violet (blue, Thermo Fisher Scientific, Boston, MA) labelled BEAS-2B cells. BEAS-2B cells were treated using $CoCl_2$ (400 μM, Sigma-Aldrich, St. Louis, MO) for 12 h and then co-cultured with iPSC-MSCs for 24 h. The number of TNTs expressed by the genetic modified iPSC-MSCs was quantified.

Immunofluorescence for CX43

BEAS-2B cells were labelled with CellTrace Violet (blue) and co-cultured with CX43-GFP-iPSC-MSCs and GFP-iPSC-MSCs. The cells were incubated with CX43 primary antibody and AlexaFluor 568 secondary antibody. The sections were counterstained with DAPI.

Overexpression of CX43 in iPSC-MSCs

For CX43 overexpression, the iPSC-MSCs were transfected using lentiviral infection as described previously (Liang et al., 2015). Briefly, the human CX43 coding sequence (Genbank: NM_000165.4) was first amplified via PCR from human 293 cell line cDNA ligated into lentivirus expression vector pGFP (Genecopoeia, Rockville, MD). pCX43-GFP and control pGFP lentivirus-based recombinant plasmids were constructed by GeneCopoeia. The pCX43-GFP and control pGFP lentivirus were packaged in 293FT cells using the 3rd generation lentiviral packaging system (Addgene, Cambridge, MA). The virus was harvested, filtered and stored. CX43 cDNA insert were sequenced for confirmation before transfection. For MSCs transfection, the viral supernatant containing a final concentration of 8 μg/mL polybrene was added into 60% confluent iPSC-MSCs. To improve transfected efficiency, multi-infections were performed. Finally, the efficiency was examined by immunofluorescence and flow cytometry.

CX43 silencing in iPSC-MSCs

CX43 in iPSC-MSCs was knockdown by using shRNA technology as previously described (Osswald et al., 2015). Three synthetic shRNAs were (pAV-U6-GFP vector, shCX43-1: 5'-AAC TGC TGG AGG GAA GGT GTG GC-3'; shCX43-2: 5'- TTT GTG TCT GTA CCC ACA CTC TT-3'; shCX43-3: 5'- GGG GTT GCT GCG AAC CTA CAT C-3') against CX43 were obtained

from Vigene Biosciences, Rockville, MD. Control cells were infected with the appropriate non-target shRNA particles. Western blot analysis was employed to examine the efficiency after transfection.

Statistical analysis

Statistical analysis was performed with SPSS software. Comparisons between more than two groups were analysed with one-way analysis of variance (ANOVA) followed by post hoc analysis or Dunnett T3 test. Independent T tests were used for comparisons between two groups. A Kruskal–Wallis rank sum test followed by a Mann–Whitney U test was utilized for comparisons of data with non-normal distribution.

Supplemental References

Aslan, H., Zilberman, Y., Arbeli, V., Sheyn, D., Matan, Y., Liebergall, M., Li, J.Z., Helm, G.A., Gazit, D., and Gazit, Z. (2006). Nucleofection-based ex vivo nonviral gene delivery to human stem cells as a platform for tissue regeneration. Tissue Engineering *12*, 877-889.

Lian, Q.Z., Zhang, Y.L., Zhang, J.Q., Zhang, H.K., Wu, X.G., Zhang, Y., Lam, F.F.Y., Kang, S., Xia, J.C., Lai, W.H., *et al.* (2010). Functional Mesenchymal Stem Cells Derived From Human Induced Pluripotent Stem Cells Attenuate Limb Ischemia in Mice. Circulation *121*, 1113-U1191.

Liang, X., Ding, Y., Zhang, Y., Chai, Y.H., He, J., Chiu, S.M., Gao, F., Tse, H.F., and Lian, Q. (2015). Activation of NRG1-ERBB4 signaling potentiates mesenchymal stem cell-mediated myocardial repairs following myocardial infarction. Cell Death & Disease *6*.

Osswald, M., Jung, E., Sahm, F., Solecki, G., Venkataramani, V., Blaes, J., Weil, S., Horstmann, H., Wiestler, B., Syed, M., *et al.* (2015). Brain tumour cells interconnect to a functional and resistant network. Nature *528*, 93-+.

Sheyn, D., Ben-David, S., Shapiro, G., de Mel, S., Bez, M., Ornelas, L., Sahabian, A., Sareen, D., Da, X.Y., Pelled, G., *et al.* (2016). Human Induced Pluripotent Stem Cells Differentiate Into Functional Mesenchymal Stem Cells and Repair Bone Defects. Stem Cell Transl Med *5*, 1447-1460.

Sheyn, D., Kallai, I., Tawackoli, W., Cohn Yakubovich, D., Oh, A., Su, S., Da, X., Lavi, A., Kimelman-Bleich, N., Zilberman, Y., *et al.* (2011). Gene-modified adult stem cells regenerate vertebral bone defect in a rat model. Mol Pharm *8*, 1592-1601.

Sun, Y.Q., Deng, M.X., He, J., Zeng, Q.X., Wen, W., Wong, D.S., Tse, H.F., Xu, G., Lian, Q., Shi, J., *et al.* (2012). Human pluripotent stem cell-derived mesenchymal stem cells prevent allergic airway inflammation in mice. Stem Cells *30*, 2692-2699.

Yao, Y., Zeng, Q.X., Deng, X.Q., Tang, G.N., Guo, J.B., Sun, Y.Q., Ru, K., Rizzo, A.N., Shi, J.B., and Fu, Q.L. (2015). Connexin 43 Upregulation in Mouse Lungs during Ovalbumin-Induced Asthma. PLoS One *10*, e0144106.

Zhang, Y., Yu, Z., Jiang, D., Liang, X., Liao, S., Zhang, Z., Yue, W., Li, X., Chiu, S.M., Chai, Y.H., *et al.* (2016). iPSC-MSCs with High Intrinsic MIRO1 and Sensitivity to TNF-alpha Yield Efficacious Mitochondrial Transfer to Rescue Anthracycline-Induced Cardiomyopathy. Stem Cell Reports *7*, 749-763.